

https://dspace.org/

A Study To Optimize Ore Evaluation At Western Deep Levels Gold Mine, Witwatersrand, By Using Geostatistics And Geological Subdivision

Braun, Rolf

2015-01-12
http://hdl.handle.net/10539/16439

Downloaded from a DSpace repository. https://dspace.org/

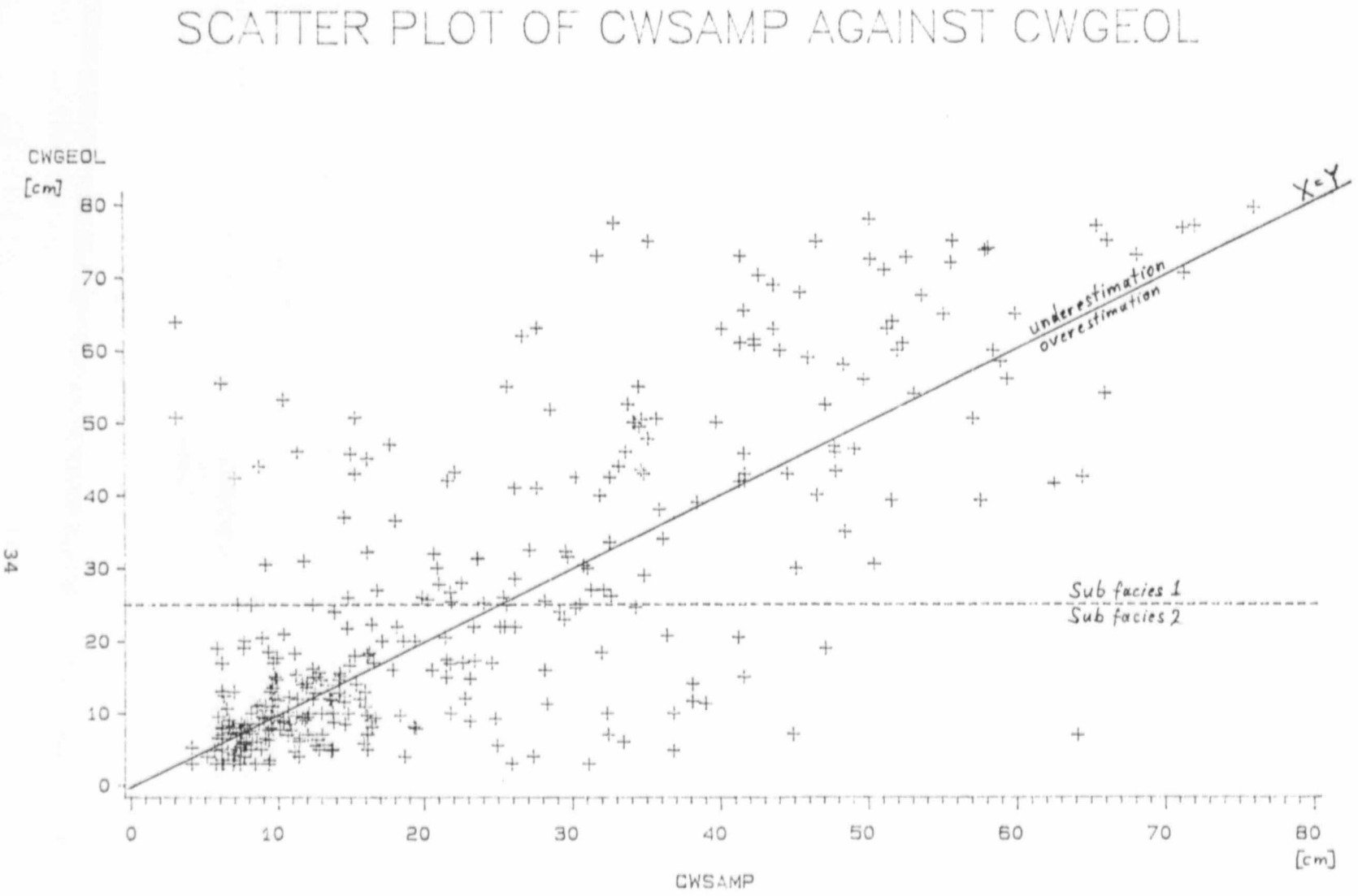


Figure 3.7: Plot of true channel width (CWgeol) against the channel width as recorded during sampling (CWsamp). Data are regularized in 25m * 25m blocks. Subfacies 1 has a true channel width of more than 25cm, Subfacies 2 of less than 25cm. For Subfacies 1 the true channel width is generally overestimated, for Subfacies 2 underestimated.

3.6.2 Facies Map

Enclosure 1 shows the subfacies distribution in the No. 3 Shaft area based on samplers' data (contours) as well as sedimertological mapping. This map forms the basis for subdivision of the study area into sedimentological homogeneous zones for the geostatistical study.

The pattern of the north - south trending Reef Type 1 ribbons or palaeochannels can clearly be recognized. Their breadth ranges from 200m to about 500m.

A confluence of two palaeochannels is responsible for the Y - shaped Subfacies 1 distribution in the northwestern part of the study area (see Enclosure 1). However, Subfacies 2 predominates here. The uniform, single conglomerate band of Reef Type 2 covers large parts of this area. There is a good agreement of the true channel width (black symbols) and the sampled channel width (green contours). In the very west, about 800m distant from the palaeochannel, the carbon seam ceases to underly the conglomerate, indicating that its occurrence might be restricted to the vicinity of the palaeo-channels.

In the southeast of the area under investigation (see Enclosure 1), at least three north - south running Subfacies 1 zones are proved by sedimentological information.

Knowledge of the different sedimentological characteristics of the two reef types proved to be valuable in an area of the central palaeochannel (see Enclosure 1; N: 650; E: 600). Here the channel width based on sampling is less than 25cm, and historical sedimentological logs also show only one thin conglomerate band. As the stopes [illegible] the area - as well as some of the historical [illegible] showed a thin shale layer above the conglomerate, it was concluded that a second conglomerate band was unexposed in the hangingwall. The historical geological information was reinterpreted (Hangingwall Quartzite changed to Internal Quartzite) and the area was defined as Subfacies 1. This proved correct later, as with mining progressing, the stope face advanced towards the edge of the channel, where the vertical distance between the two conglomerate bands decreases (see Fig. 3.4). Therefore the top conglomerate band became exposed again within the stoping width. After digitizing of the sample data it also became obvious that this area lies in the course of a palaeochannel, and 200m to the north both reef bands were exposed, resulting in a channel width of more than 100cm.

Just west of the palaeochannel which appears to be the continuation of the one from the northwestern study area (see Enclosure 1), the subfacies distribution is uncertain. No geological data is available here, and the sampling data show isolated patches of thick next to thin channel width.

The choice is to assume this area as being Subfacies 1, explaining the patches of thin channel width as areas where reef was left in hangingwall; or assuming the region to be of Subfacies 2 - type. Then patches of thick channel width represent areas where Footwall - pebble bands were sampled as well.

This area is excluded from the geostatistical analysis because of this uncertainity.

4 Geostatistical Study

4.1 Present mine valuation technique

As the Carbon Leader Reef is a tabular deposit, it is treated as a two - dimensional orebody. This requires working with accumulations. To calculate accumulations, the assaying result of each sample is multiplied by its sampling width, giving a cm*g/t value. These data are added up for each sampling section to give the accumulation, i.e. concentration of gold per unit area at this point of the two - dimensional reef surface (Storrar, 1977). This is basically a weighting of each assay value by its sample width. Figure 4.1 shows an example of such a calculation.

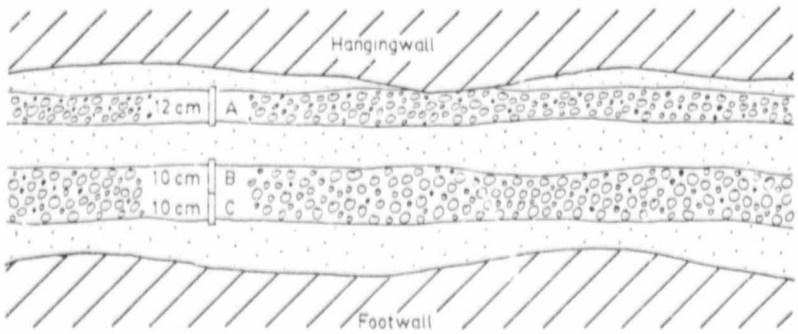


Figure 4.1: Calculation of accumulation in multiple reef band area. Two conglomerate bands are exposed. Three samples are taken. The assaying results are:

A: 79.8 g/t
B: 54.9 g/t
C: 179.8 g/t

The accumulative grade is: (12cm * 79.8g/t) + (10cm * 54.9g/t) + (10cm * 179.8 g/t) = 3305cm*g/t.

Ideally, the individual samples should not only be weighted by their sample length, but also by their density. However, because of the minimal percentage of metal and no wide variation of other heavy minerals highly correlated with gold, the density can be accepted as equal for all samples.

The first step of the valuation procedure as currently applied at Western Deep Levels Gold Mine is to cover the whole mine area with a fixed $(100m)^2$ grid. This grid is tilted -15 degrees against true North so as to have its rows along the average strike and its columns along the average dip of the strata (pers. comm., I. Dohm).

In the mined out area the arithmetic average of all the arithmetic averages of the gold assay data (cm*g/t) per stope face within each $(100m)^2$ block is assigned to the center of this block as its true block value. Then semivariograms are calculated on these data blocks. Except for the north - south directions, they show a pure nugget effect, therefore only data blocks north and south of an oreblock are used in the estimation of this oreblock. The area under investigation is then subdivided into the four quadrants centered at the No. 3 Shaft. The arithmetic row averages in those quadrants decrease downdip, so that, if row numbers are plotted

against their average cm*g/t values - starting from the north -, they decrease exponentional as shown in Figure 4.2.

Due to this trend of the data an estimation of an unmined ore block of $(100m)^2$ from its northern (or southern) adjacent mined out blocks seems possible. As semivariograms of $(100m)^2$ block values in a North - South direction show ranges of 700m, up to seven data blocks are used to estimate an unmined block.

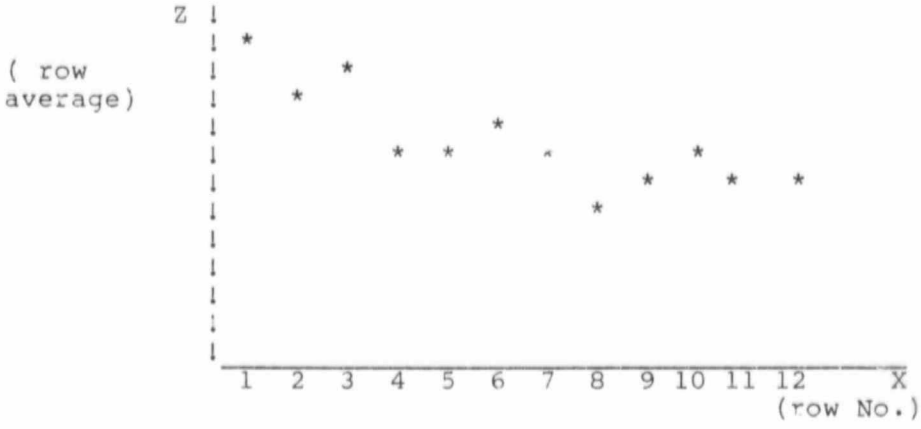


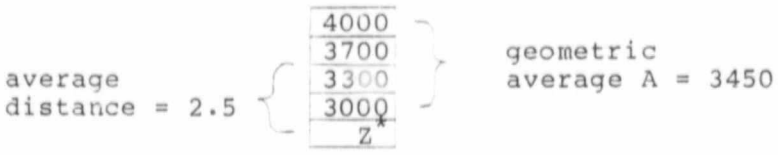
Figure 4.2: Exponentional decrease of row average cm*g/t values from North (left) to South (right).

The formula used for estimation expresses the relationship of gold content and position as shown in Figure 4.2:

$$Z^* = A * \exp(bX)$$

with Z^*: block estimate
A: geom. mean of up to seven blocks in column
b: slope factor defining the shape of the curve
X: average row distance of data blocks to the block to be estimated.

An example will make this procedure clearer: assume that a block is to be estimated from four data blocks in the North with the following configuration:



The estimate Z^* then becomes:

$$Z^* = 3450 * \exp(b*2.5)$$

Assuming a slope factor of -0.13, $Z^* = 2493$ cm*g/t.

For the annual ore reserve estimation , the gold content of the (irregularly) shaped ore reserve blocks to be mined are then calculated as an average of the $(100m)^2$ block estimates they cover, weighted by area:



average of shaded area:

$.125*Z^*_1 + .250*Z^*_2 + .250*Z^*_3$
$+ .250*Z^*_4 + .125*Z^*_5$

This procedure is reported as working to the satisfaction of the mine in the southern quadrants, but gives poor results in the northwestern quadrant, as no exponential regression line which fits the data well can be established for this area.

4.2 Comparison of different Estimation Techniques

Ore estimation is done to have grade estimates of ore blocks before these are mined.

If the estimates are perfect, the estimated grade of each ore block will be equal to the true grade, so their difference will be zero.

A linear regression of the true grade Z as dependent variable on its perfect estimate Z^* will give a regression formula with a slope of 1.0 and an intercept of 0:

$$Z = 0 + 1.0 * Z^* \qquad (1a)$$

For lognormally distributed variables this becomes:

$$\ln(Z + b) = 0 + 1.0 * \ln(Z^* + b) \qquad (1b)$$

where b is the additive constant (Krige, 1951).
As then $Z^* = Z$ for each pair, their difference is zero, and the variance of the differences is zero:

$$Z^* - Z = 0 \qquad (2)$$

Furthermore, the mean values of the two variables are the same:

$$\overline{Z}^* = \overline{Z}$$

None of today's estimation techniques gives this perfect knowledge. However, the quality of different techniques can be compared with the 'perfect' position using the above mentioned criteria. This is done in the following investigation.

Criterion 1 will be the slope of the regression of Z on Z^*. A slope close to 1.0 ensures what is known as 'conditional unbiasedness', meaning that there is no systematic over- or underestimation in certain grade categories (Krige, 1951).

Criterion 2 will be the variance of the differences of $(Z^* - Z)$, which is the estimation or error variance. The smaller this variance is, the closer the estimates are to reality. In order to compare normal and lognormal kriging, normal variances are transformed into lognormal variances. From the relatonship:

$$V^2 = \overline{Z}^2 * [\exp(LV^2) - 1] \qquad (3)$$

the lognormal variance can be calculated as (Krige,1981):

$$LV^2 = \ln\left[\frac{V^2}{\overline{Z}^2} + 1 \right]$$

with:
V^2 = Population Variance
LV^2 = Lognormal Variance
$\overline{Z}$ = Population Mean

In the case of lognormal kriging using a three parameter lognormal model ($b \neq 0$), and where the additive constant varies from area to area the lognormal variance has to be corrected for the additive constant, otherwise these variances can not be compared on the same basis. The relationship:

$$\overline{Z}^2 * [\exp(LV^2) - 1] = (\overline{Z} + b)^2 * [\exp(LV_b^2) - 1]$$

gives:

$$LV^2 = \ln\left(\frac{(\overline{Z}+b)^2 * [\exp(LV_b^2) - 1]}{\overline{Z}^2} + 1\right) \qquad (4)$$

where LV_b^2 is the lognormal variance of the three parameter model and LV^2 is the corresponding logarithmic variance of a two-parameter model with the same variance on an untransformed basis.

Criterion 3 is a comparison of the mean values for true data and estimates. Any valid estimation method should ensure that the mean of all the estimates is equal to the mean of the true data, otherwise global over- or underestimation occurs. Equal means thus guarantee global unbiasedness. The difference in the means is equal to the average error ($Z^* - Z$) of the estimation, which ideally is zero.

Ore blocks are not mined and milled individually, therefore their true grades are never known. In this study the average of all samples taken inside an ore block after it has been mined is taken as its true grade, provided the number of samples is large enough (see Appendix 1.1). This true value is compared with its estimate, which is based on the data available before the ore block was mined.

4.3 Comparison of Mine Estimates with True Data

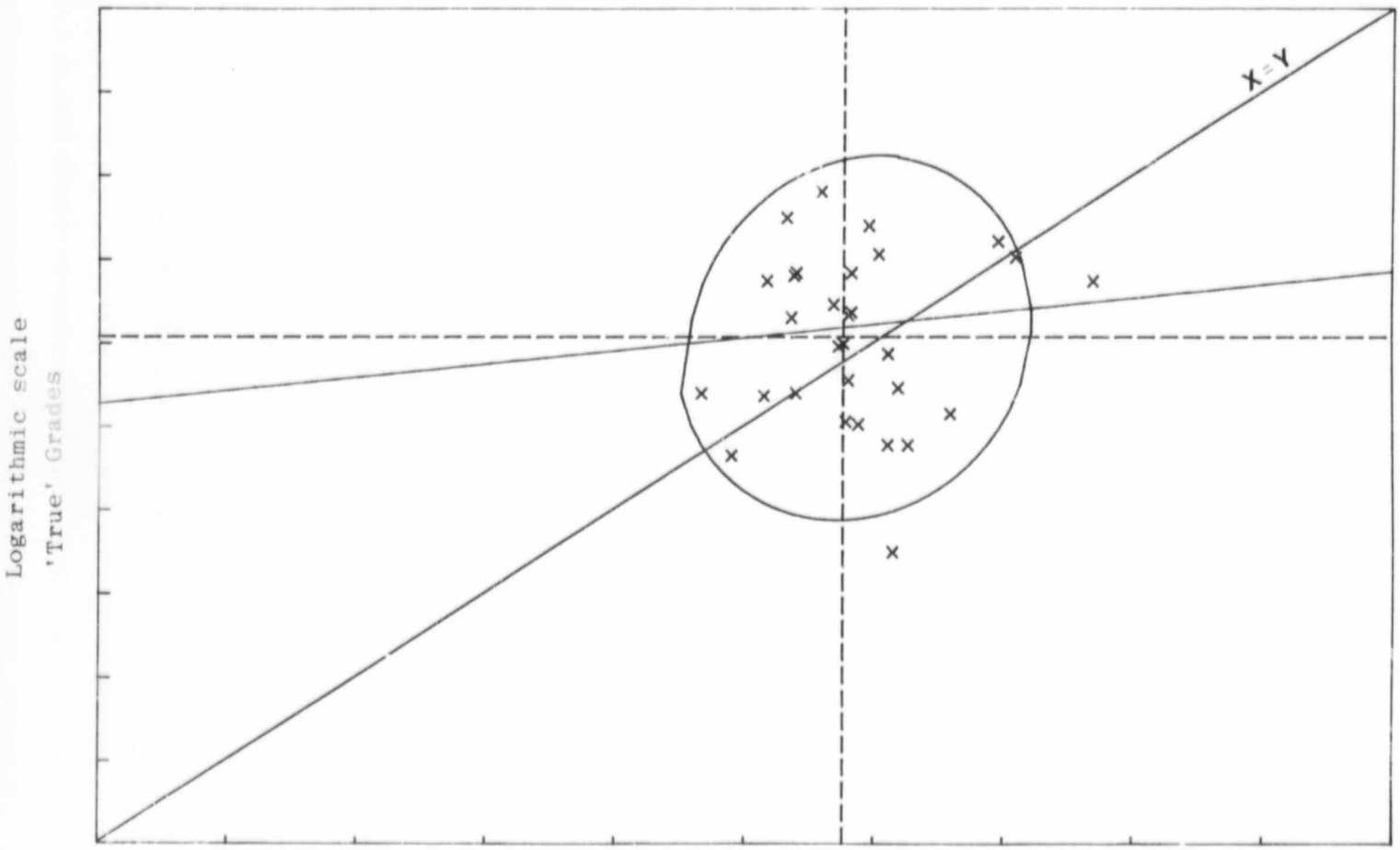
Ore reserve estimation at Western Deep Levels Gold Mine has been done since 1981 on the basis as described in section 4.1.

For 86 of all ore blocks estimated since then, sufficient follow - up data were available to be compared with their estimates. 30 of them lie in the northwestern quadrant for which no exponential regression line could be established by the mine. The remaining 56 are from the southern quadrants. A further 67 blocks were delimited in the mined out areas of the southern quadrants and their grades were estimated by the author using the mine method, giving a total of 123 blocks for the southern quadrants. This could not be done in the upper quadrant, as the mine estimates in this quadrant involve personal judgement (pers. comm. H.Elliot).

The northeastern quadrant of the shaft area is not included in this analysis, as it has been mined out totally, and no geological information is available there.

Figure 4.3 shows a regression plot of the 30 data pairs from the northwestern quadrant.

Fig.4.3:Regression Diagram Mine Method NE-Quadrant
n=30



The 'true' grades are plotted along the vertical axis, their estimates along the horizontal axis. In addition to the pairs, the line X=Y, the regression line of the 'true' grades on their estimates, the means of the marginal distributions (dashed lines), and the ellipse enclosing 90% of the data points is shown.

The lognormal regression formula is (add. constant is 170cmg/t):

$$\ln(Z + 170) = 7.1 + 0.16 * \ln(Z^* + 170)$$

the logarithmic estimation variance , corrected for the additive constant:

$$LV_e^2 = 0.1280$$

and the difference in the means ($\bar{Z}^* - \bar{Z}$) is:

$$\bar{Z}^* - \bar{Z} = -356 \text{ cmg/t}$$

These results show that with a slope of the regression line of only 0.16 the procedure is strongly conditionally biased and gives severe underestimations in the lower grade categories and overestimations in the upper grade categories.

A regression analysis for the two quadrants in the southwest of the area under investigation (No. of blocks = 56) reveals that the results here also can be improved (see Figure 4.4). The regression formula is:

$$\ln(Z + 170) = 3.2 + .61 * \ln(Z^* + 170) \quad ;$$

with a logarithmic estimation variance of:

$$LV_e^2 = .1721$$

and a difference in the means of:

$$\bar{Z}^* - \bar{Z} = -288 \text{ cmg/t}$$

The regression analysis of the 67 simulated data pairs is:

$$\ln(Z + 170) = 3.7 + .56 * \ln(Z^* + 170) \quad ,$$

the logarithmic estimation variance, corrected for beta:

$$LV_e^2 = .1858$$

The difference in the means is:

$$\bar{Z}^* - \bar{Z} = -590$$

This leads to the conclusion that the method presently applied - as far as known, only at this mine - does not really give good results, even in areas where exponential regression lines can be fitted to the row averages. The author therefore cannot recommend this method.

An analysis on the combined data for the southern quadrants (n = 123), is shown in Figure 4.5 . The results are:

Regression formula:

$$\ln(Z + 170) = 3.5 + .59 * \ln(Z^* + 170)$$

Logarithmic estimation variance, corrected for the additive constant:

$$LV_e^2 = .1801$$

Difference in means:

$$Z^* - Z = -450 \text{ cmg/t}$$

The consistent underestimation of the global mean grade is probably due to the fact that a type of weighted geometric mean of the up to 7 data blocks north (or south) of the ore block rather than a weighted arithmetic mean or a weighted Sichel's t-estimator is used in the estimation formula.

Fig.4.4:Regression Diagram Mine Method S - Quadrants
n=56

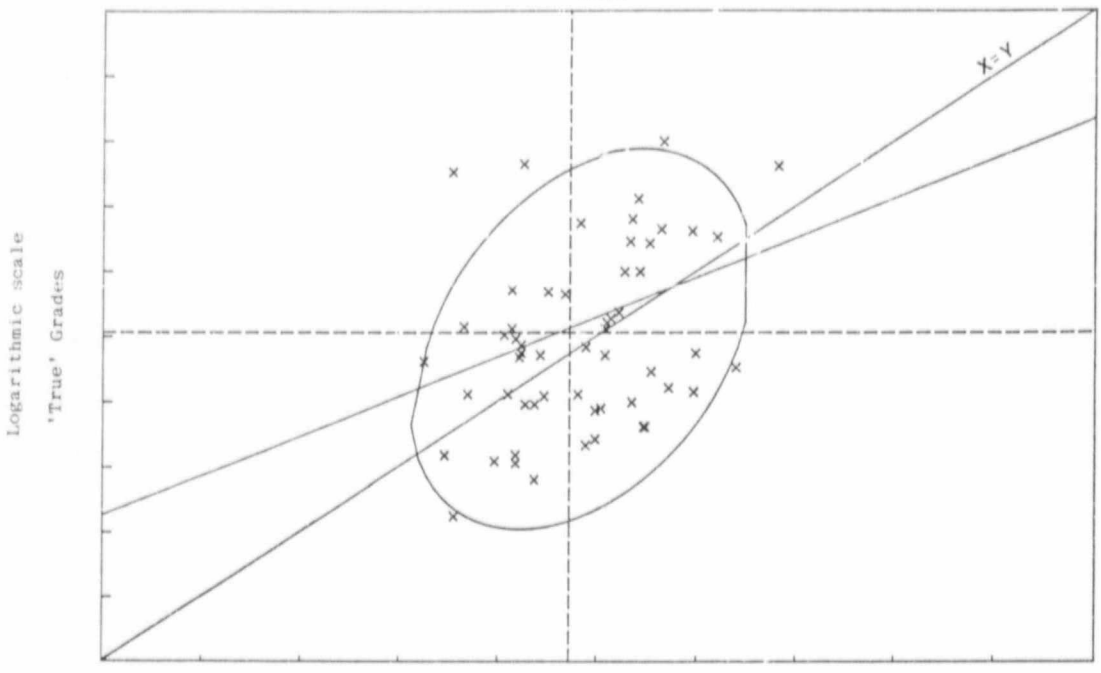
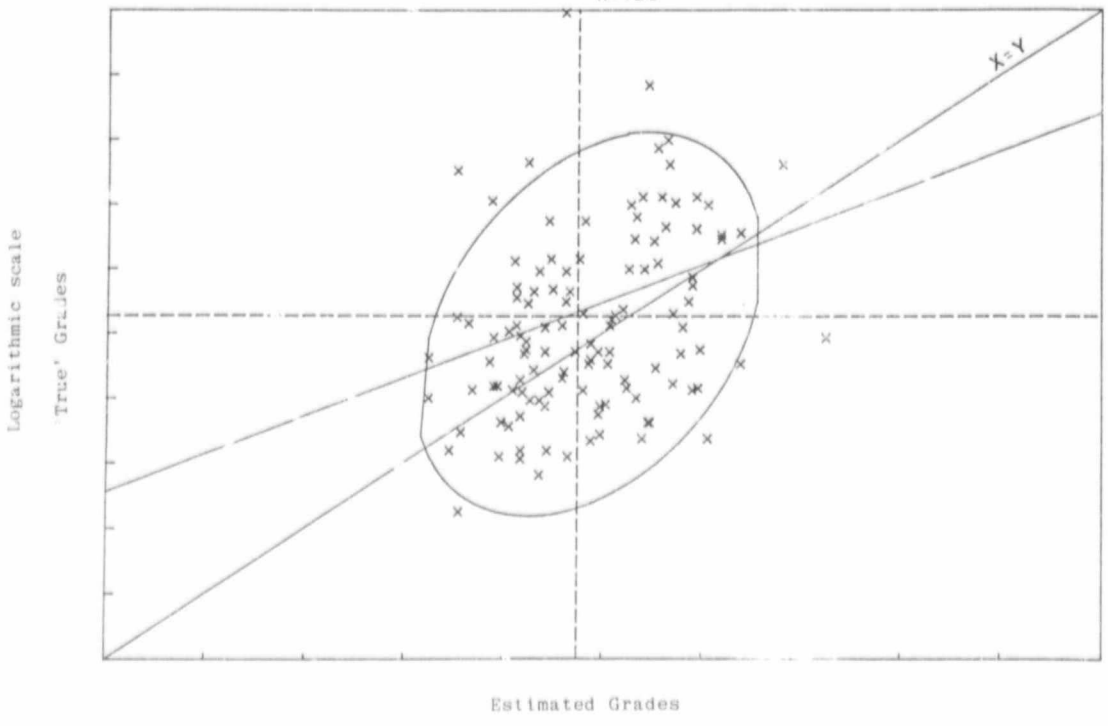


Fig.4.5:True and Simulated Mine Estiates S - Quadrants
n=123



4.4 Assay Data

4.4.1 Collection

When this study commenced, none of the individual assay data in the area under investigation was digitized. Only the averages of $(100m)^2$ blocks as described under 4.1 were available on a data base.

After development of the neccessary software (see Appendix 2.2), copies of the mine assay plans were digitized. The stope sheet coordinates were converted to horizontal coordinates, using the author's program 'CONVERT'(see Appendix 2.3). The resultant plans contain the gold grade, the channel width and the stoping width, and for about 70% of the data points the samples were assayed for uranium as well. The resulting data base then consisted of the two coordinates in the horizontal plane as independent variables and the dependent variables uranium (cmkg/t,if assayed), gold (cmg/t), channel width(cm) and stoping width (cm).

All available data have been digitized. As a few assay plans were missing, this has resulted in holes in the data coverage for some of the areas in the northwestern quadrant, but in general the information available covers all of the mined out area in the No. 3 Shaft area (except the northwestern quadrant).

Samples were taken at 5m intervals along stope faces, and each stope was ideally visited once per month. With an average stope advance of 10m per month this has resulted in a pseudoregular sample grid of 10m by 5m.

4.4.2 Analysis

After digitizing, gold data at 36160 'points' were available for analysis. Because of the small support of the chip samples (Storrar, 1977) they are considered as point samples. These data follow a three - parameter lognormal distribution model (Krige, 1960) with an additive constant of 170 cmg/t. The calculated skewness of the logtransformed distribution $Y = \ln(Z + 170)$ is zero and the lognormal variance is 1.035. The mean grade (after adding a constant to allow comparison, but not to disclose the true data) is 5419 cmg/t. Figure 4.6 shows the grouped data plotted on lognormal probability paper (using program 'PROBPLOT', developed by the author, see Appendix 2.4).

The spatial structure of the data was analysed by means of the semivariogram. The merits and characteristics of the semivariogram are well documented (e.g. Matheron,

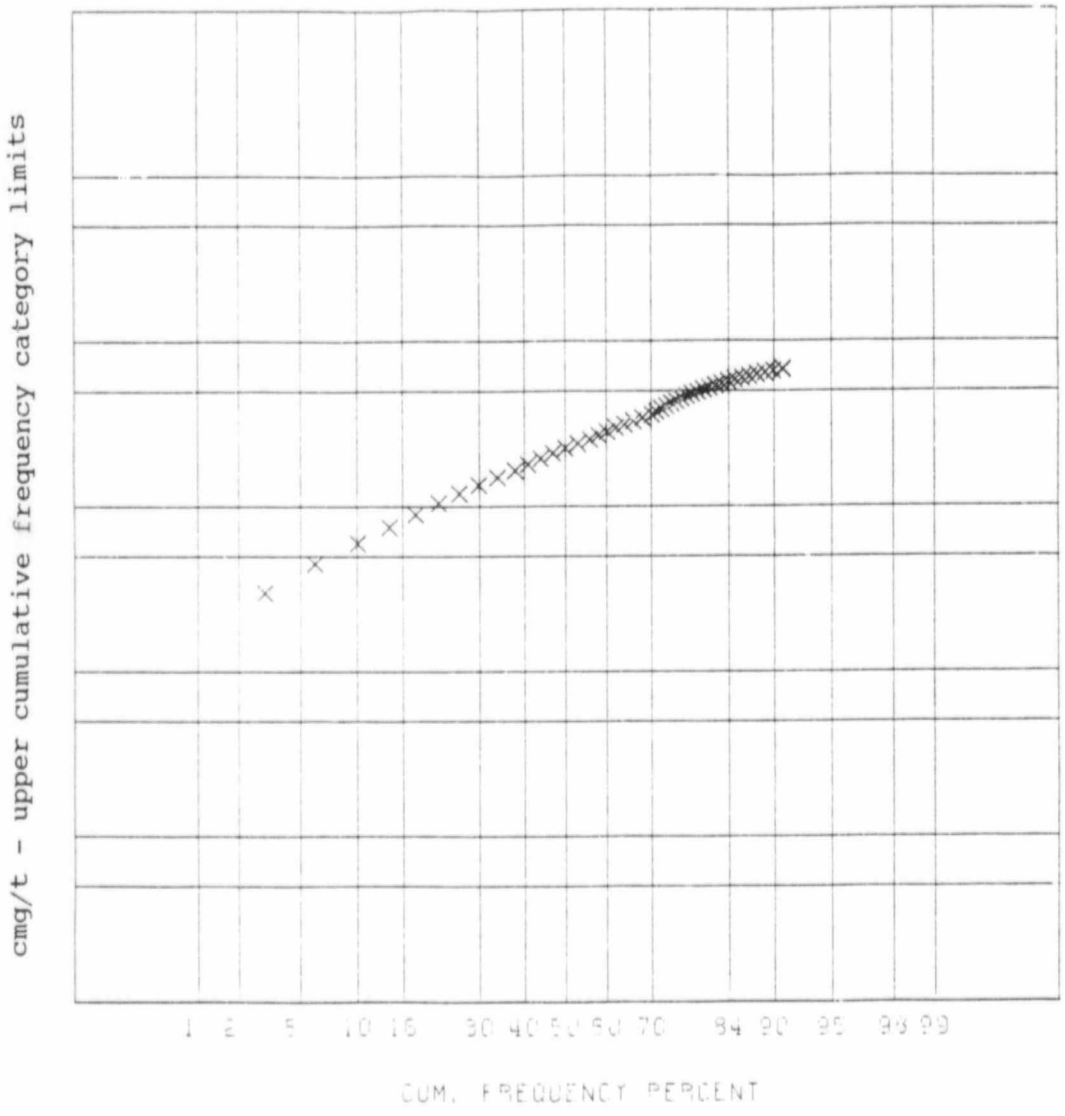


Figure 4.6: Logarithmic probability plot of all data.

1963; Journel & Huijbregts, 1978), and will not be repeated here. A short description of the semivariogram estimators used is given in Appendix 1.2.

Directional logtransformed semivariograms were calculated on the data. Using logtransformed semivariograms has the advantage of reducing the effect of outliers (Krige & Magri, 1982). Also the validity of logtransformed semivariograms can easily be checked with the variance - size of area relationship (Krige, 1981).

The overall sill of these logtransformed semivariograms is the same in all directions, and equals the logarithmic variance of the data. The ranges depend on the direction in which the semivariogram is calculated. This kind of anisotropy is termed geometric (e.g Journel & Huijbregts, 1978). It is the common type of anisotropy found in the Witwatersrand gold reefs (e.g. Krige et al, 1969; Janisch, 1986).

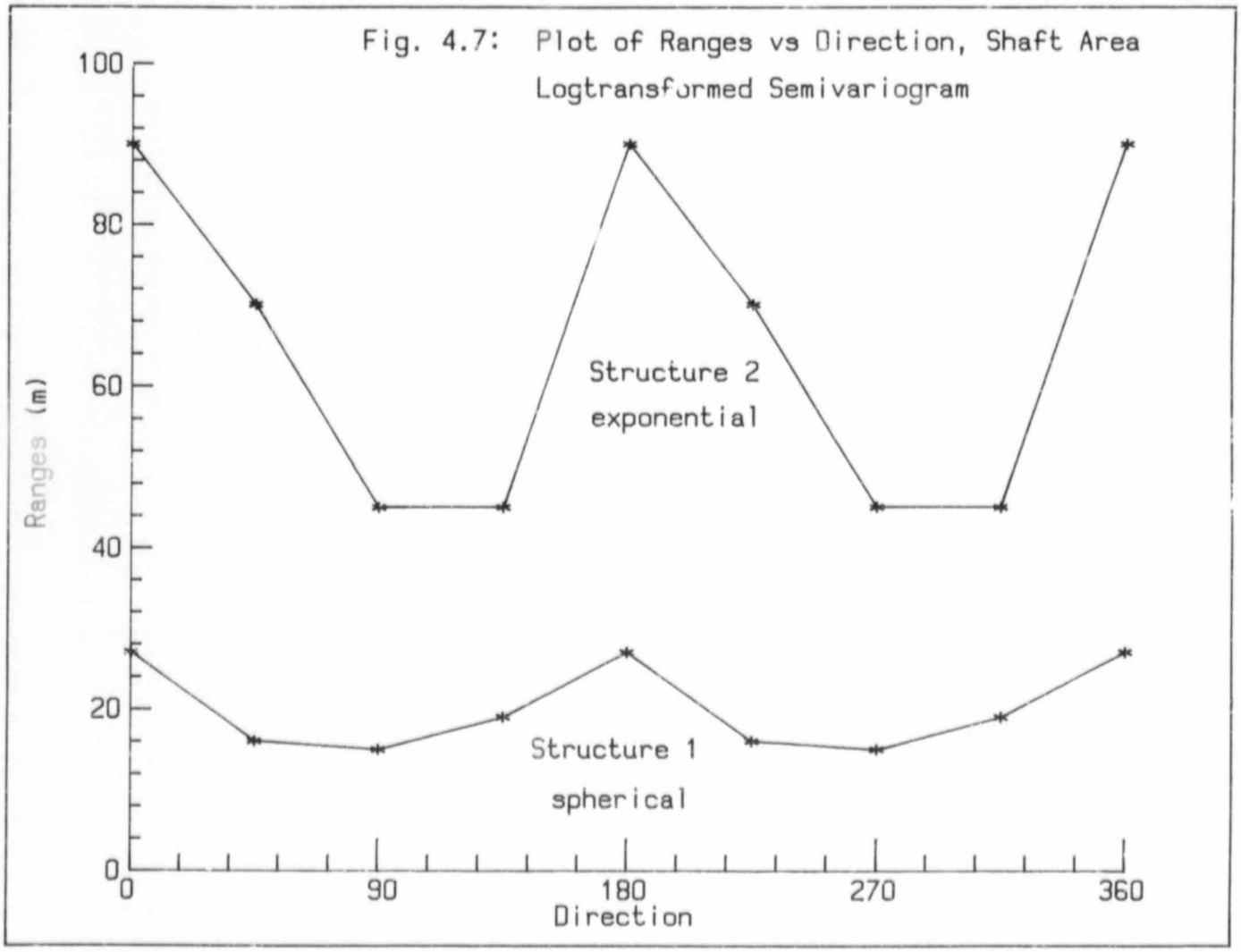
A model consisting of a nugget effect, a spherical and an exponential structure can be fitted to the experimental logtransfomed semivariograms. The range of the nugget effect is zero. A plot of the ranges of the spherical structure 1, and the exponential structure 2 against the direction shows that for both the direction of maximal variation is approximately east -

west, that of minimal variation north - south (Fig. 4.7). This closely agrees with the sedimentology and the north - south running palaeochannels, which distributed the gold more evenly in the flow direction than across. Figure 4.8 shows the two calculated logarithmic semivariograms in these main directions, and the fit of the model. The anisotropy factors for the east - west direction are 1.8 for structure 1 (spherical), and 2.0 for structure 2 (exponential).

The validity of the lognormal model was checked with the variance - size of area relationship (Krige, 1981). From the available data the average logarithmic variance of a point sample in a block can be calculated for any blocksize by taking the logarithmic variance of the samples in the block for each block of that size, multiplying it by its degrees of freedom, and summing it up. This sum is then divided by the sum of the degrees of freedom (e.g. Rendu, 1978). In formula form this reads:

$$\overline{LV^2}_{S \text{ in } B} = \frac{[(n-1) * LV^2_{S \text{ in } B}]}{(n-1)} \qquad (5)$$

with: S: Sample
B: Block
LV^2: Variance
n: Number of samples


Fig. 4.7: Plot of Ranges vs Direction, Shaft Area
Logtransformed Semivariogram
Ranges (m)
100
80
60
40
20
0
Structure 2
exponential
Structure 1
spherical
0
90
180
270
360
Direction

This is repeated for different block sizes. If the average logarithmic variance is plotted against the logarithm of the area, the data closely follow a straight line. The logarithmic block variance can be read off the graph as the difference between the total sample variance (dashed line on Figure 4.9), and the variance of the samples inside a block.

This average logarithmic variance is equal to the average semivariogram value for each specific block size (e.g. Journel & Huijbregts, 1978). A valid semivariogram model will be closely related to the variance - size of area graph.

Figure 4.9 shows the variance - size of area graph calculated experimentally on the data (by using formula 5), and the corresponding values calculated theoretically from the logtransformed semivariogram of the sample values, both for block sizes of $(12.5m)^2$, $(25m)^2$, $(50m)^2$ and $(100m)^2$. The difference in no case exceeds 2.5%. This indicates that the fitted semivariogram model is a good representation of the gold mineralisation.

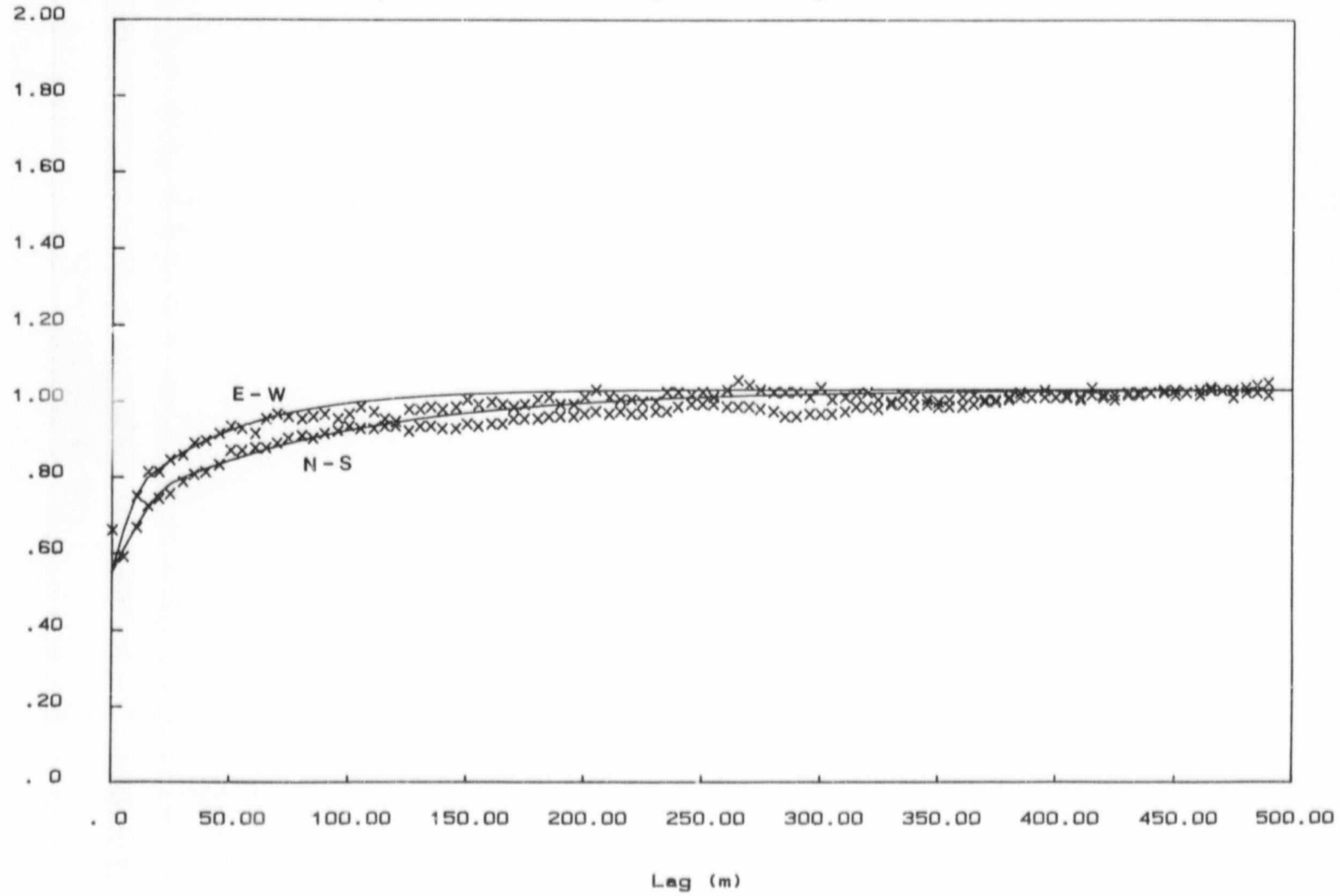
Both Hawkins & Cressie - transformed (Hawkins & Cressie, 1980) and backtransformed semivariograms (Armstrong, 1984) are shown in Figures 4.10 and 4.11. The backtransformed semivariogram is derived from the

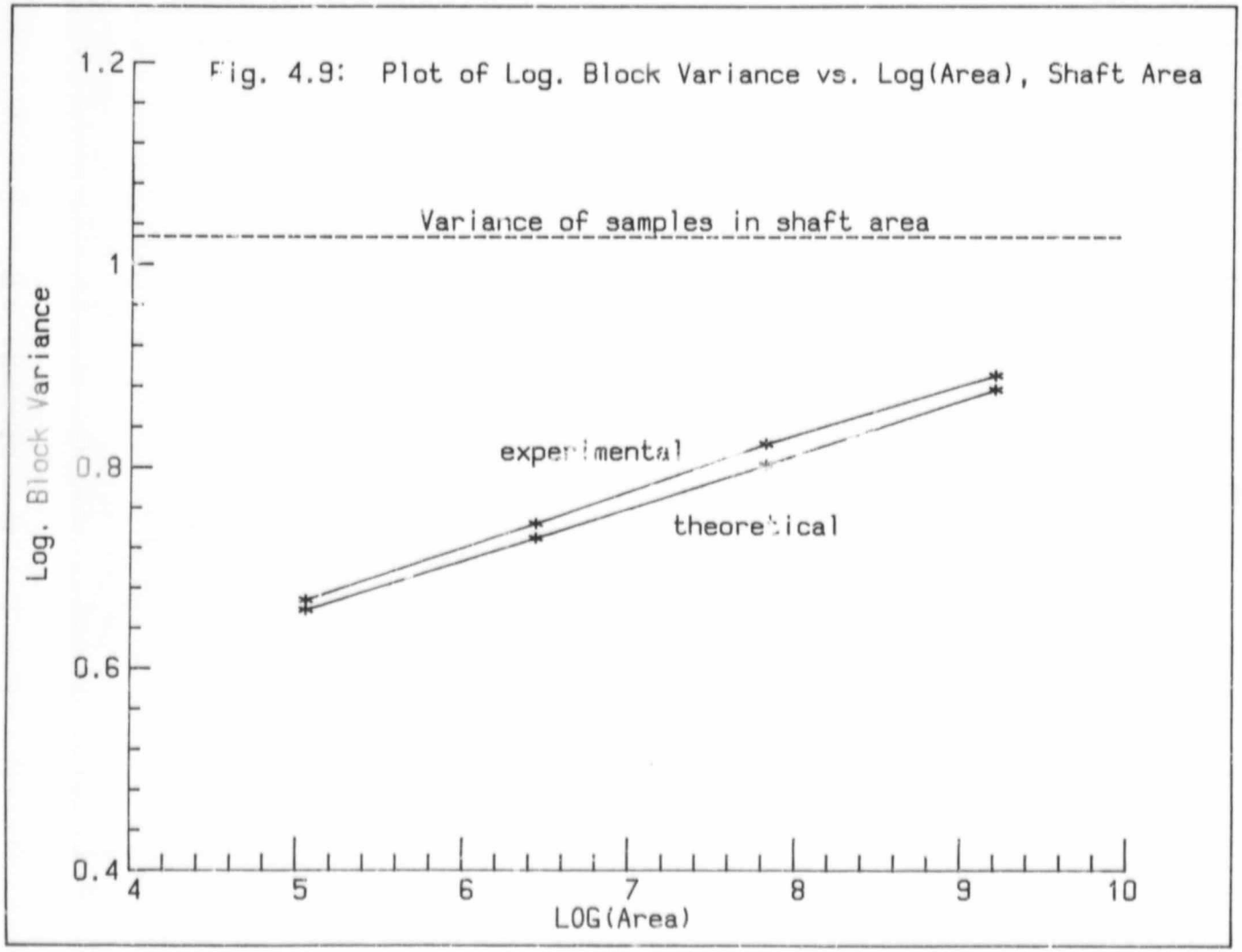
logtransformed semivariogram, and is therefore not fitted directly to any experimentally calculated semivariogram values.

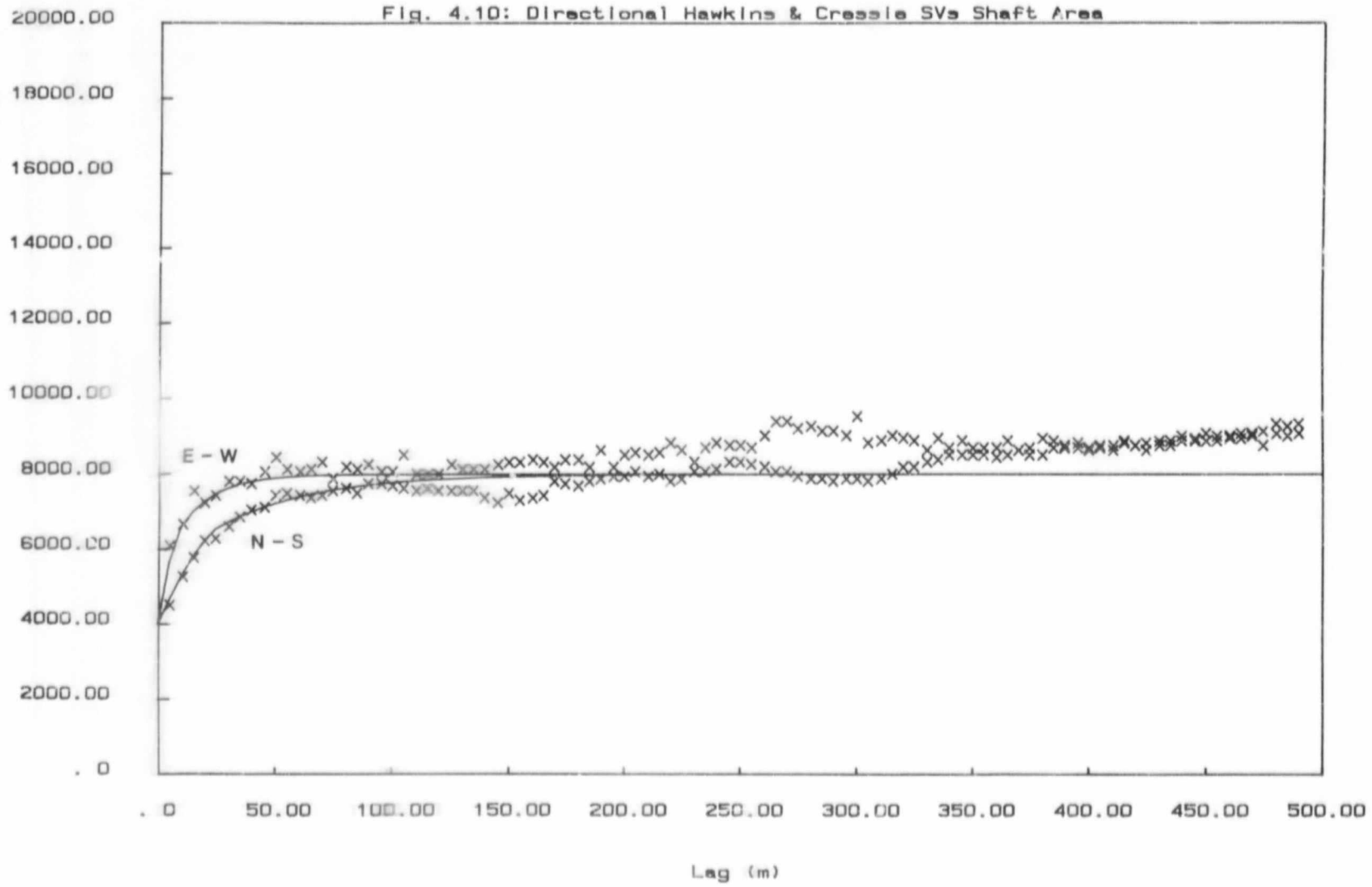
A nested structure of a nugget effect, a spherical and an exponential model is fitted to the Hawkins & Cressie transformed semivariogram. The ranges of the second, exponential structure, are shorter than those of the logtransformed semivariograms (Fig. 4.10).

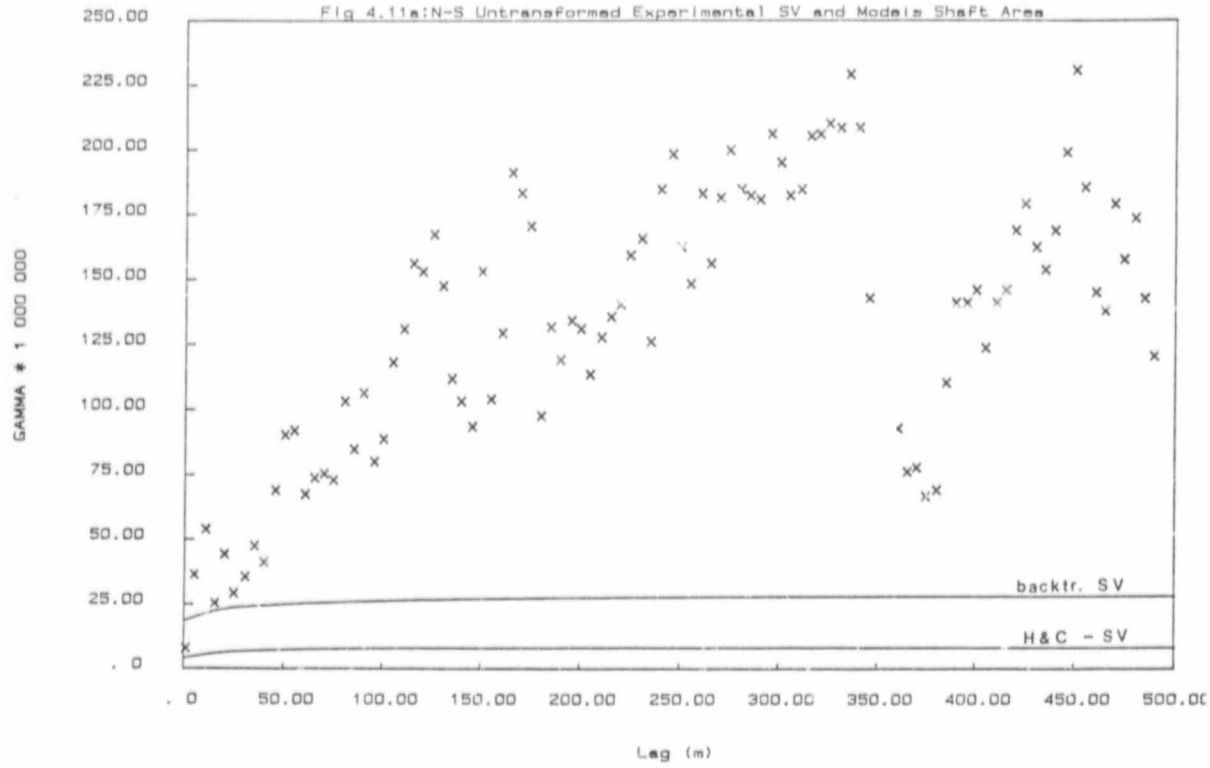
The differences between the backtransformed model and the Hawkins & Cressie model, and the standard semivariogram estimator clearly show the effect outliers have on the standard semivariogram estimator (Fig. 4.11a and b). The untransformed variance of the data including all outliers (V^2 = 104 603 008) is more than 4 times the backtransformed variance (V^2 = 25 880 104), which is calculated using formula (3).

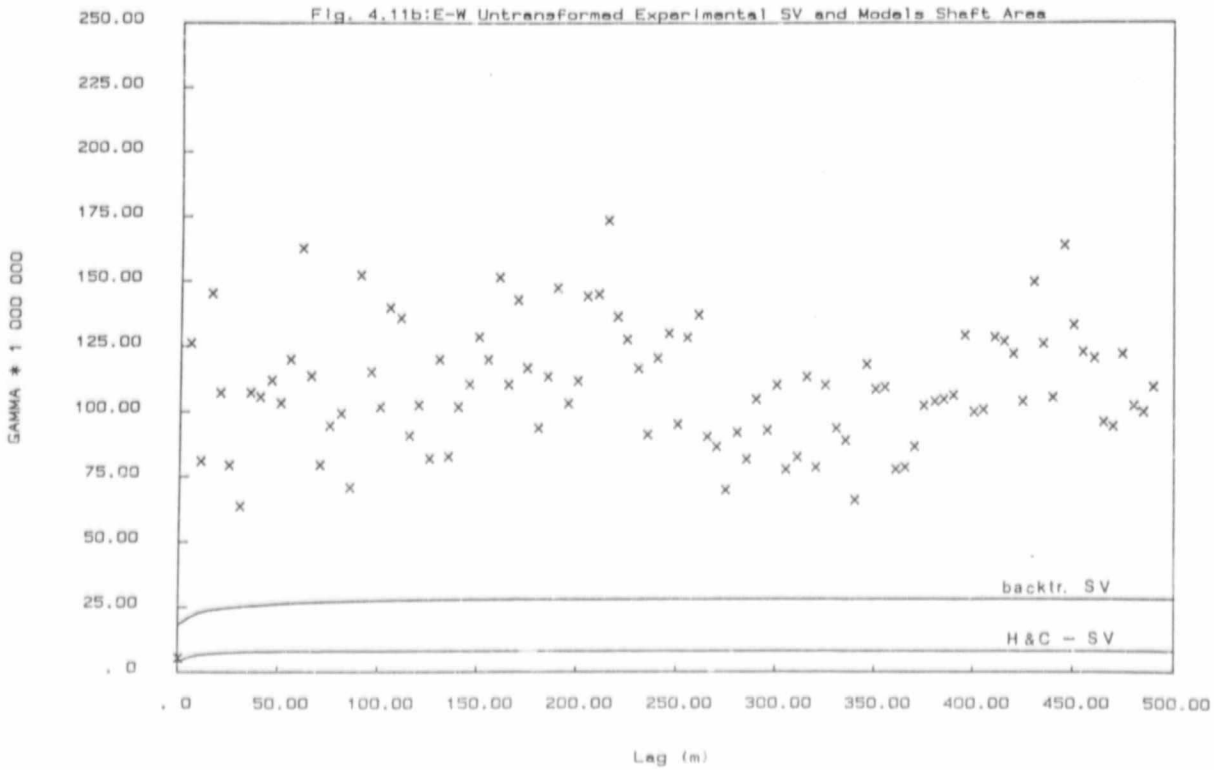
Fig 4.8: Directional Log. Semivariograms of Shaft Area




Fig. 4.9: Plot of Log. Block Variance vs. Log(Area), Shaft Area
Variance of samples in shaft area
experimental
theoretical
Log. Block Variance
LOG(Area)
1.2
1
0.8
0.6
0.4
4
5
6
7
8
9
10


Fig. 4.10: Directional Hawkins & Cressie SVs Shaft Area
GAMMA * 1 000
20000.00
18000.00
16000.00
14000.00
12000.00
10000.00
8000.00
6000.00
4000.00
2000.00
. 0
E - W
N - S
. 0
50.00
100.00
150.00
200.00
250.00
300.00
350.00
400.00
450.00
500.00
Lag (m)


Fig 4.11a:N-S Untransformed Experimental SV and Models Shaft Area
GAMMA * 1 000 000
250.00
225.00
200.00
175.00
150.00
125.00
100.00
75.00
50.00
25.00
. 0
backtr. SV
H&C - SV
. 0
50.00
100.00
150.00
200.00
250.00
300.00
350.00
400.00
450.00
500.00
Lag (m)


Fig. 4.11b:E-W Untransformed Experimental SV and Models Shaft Area
GAMMA * 1 000 000
250.00
225.00
200.00
175.00
150.00
125.00
100.00
75.00
50.00
25.00
. 0
backtr. SV
H&C - SV
. 0
50.00
100.00
150.00
200.00
250.00
300.00
350.00
400.00
450.00
500.00
Lag (m)

4.5 Geostatistical Estimation of Mine Ore Blocks, without subdivision

4.5.1 Regularisation of sample data and analysis of regularized data

As a simulation of an ore reserve estimation based on more than 36000 data reaches towards the limits of even a mainframe computer, the data were regularized. The $(100m)^2$ grid used by the mine so far seemed to be rather wide, so the data were regularized on a $(50m)^2$ grid, using the author's program 'DATABLOK' (see Appendix 2.5).

Only data blocks containing more than a certain number of samples are included in the analysis. The procedure to define the minimum number of data points in a block to warrant inclusion in the analysis, is described under Appendix 1.1.

A lognormal probability plot of these $(50m)^2$data blocks is shown in Figure 4.12. An additive constant of 170 cmg/t gives a skewness of zero, a mean of 5433 cmg/t, and a logarithmic variance of 0.287. Lognormality is preserved.

Semivariograms of the data blocks calculated in the two main directions of anisotropy show that a model can

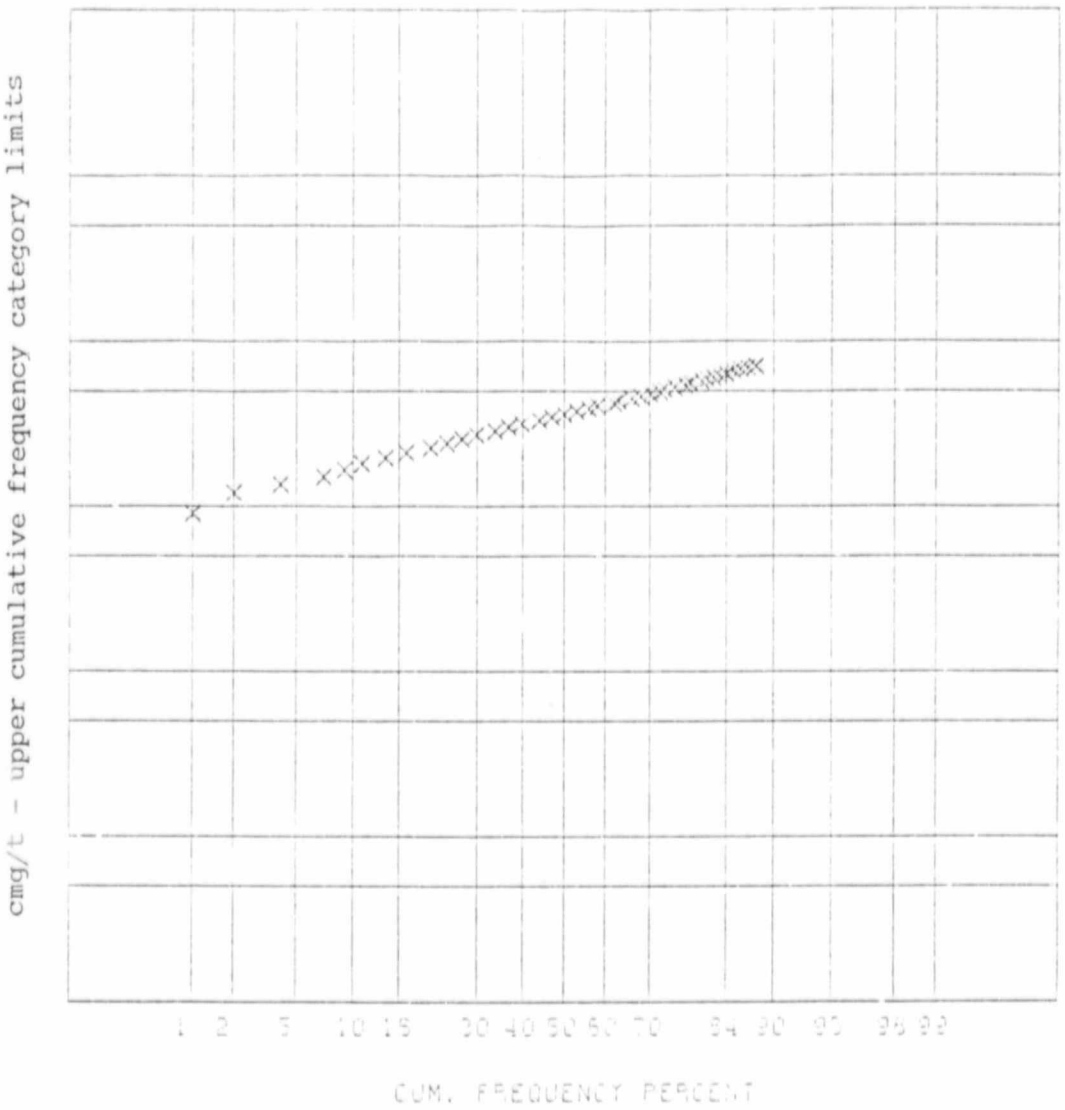


Figure 4.12: Logarithmic probability plot of regularized $(50m)^2$ data blocks.

easily be fitted to the north - south direction (Fig. 4.13a). In the east - west direction it is difficult to find a suitable model for the calculated semivariogram values, and it is understandable that the mine assumes a pure nugget effect for their regularized data in this direction. However, the modelling is complicated because of the small number of data, which is 1206 compared to 36160 for the point data. The model finally fitted in the east - west direction is based on the north - south model and the anisotropy factors found for the point data (Fig. 4.13b).

Figures 4.14a,b show the models fitted to the Hawkins and Cressie transformed semivariograms. The back-transformed semivariogram is calculated from the logtransformed semivariogram model (see Appendix 1.2). Figure 4.15a and b show the models of the back-transformed, and Hawkins & Cressie transformed semi-variograms, and the experimental semivariograms for untransformed data. The deviation of the calculated points again shows the distortion outliers impose on the standard semivariogram estimator.

The semivariogram model based on the Hawkins & Cressie transformation has the same relative nugget effect as the logtransformed semivariogram (28%), whereas the backtransformed semivariogram has a relative nugget

Fig. 4.13a: N-S (50m*50m) Data Blocks SV Shaft Area

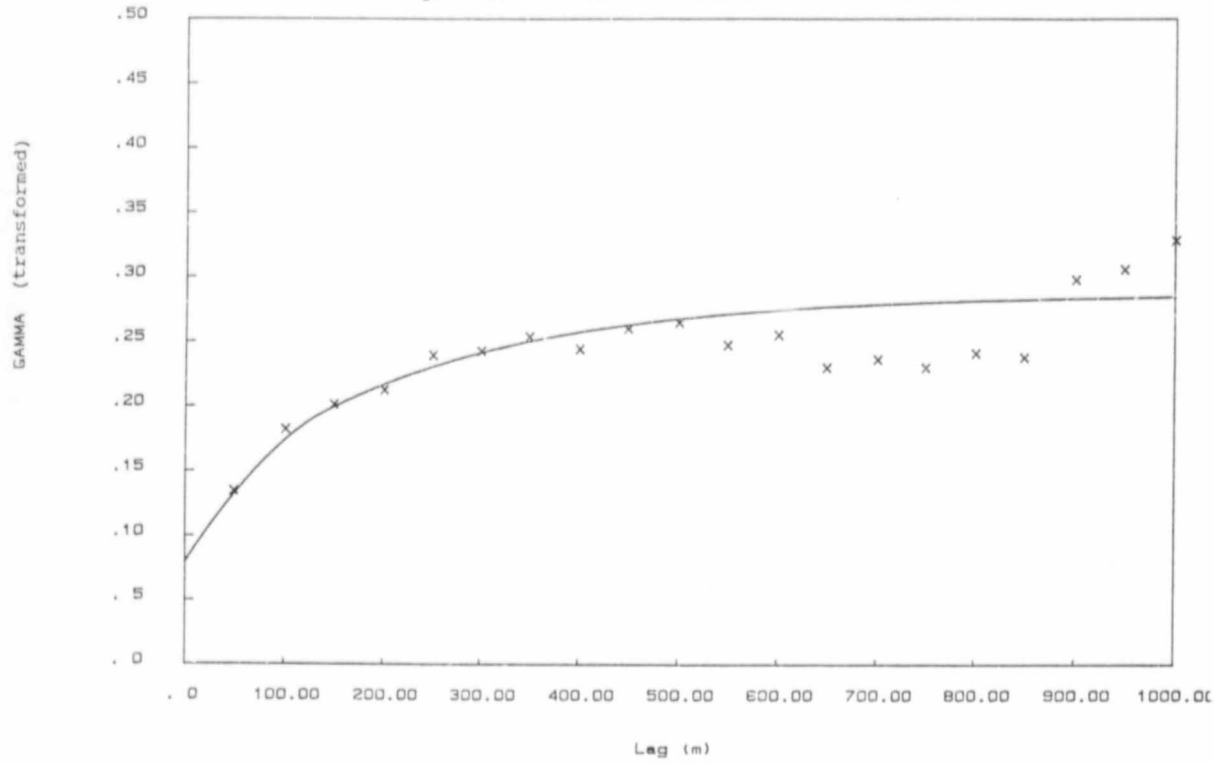
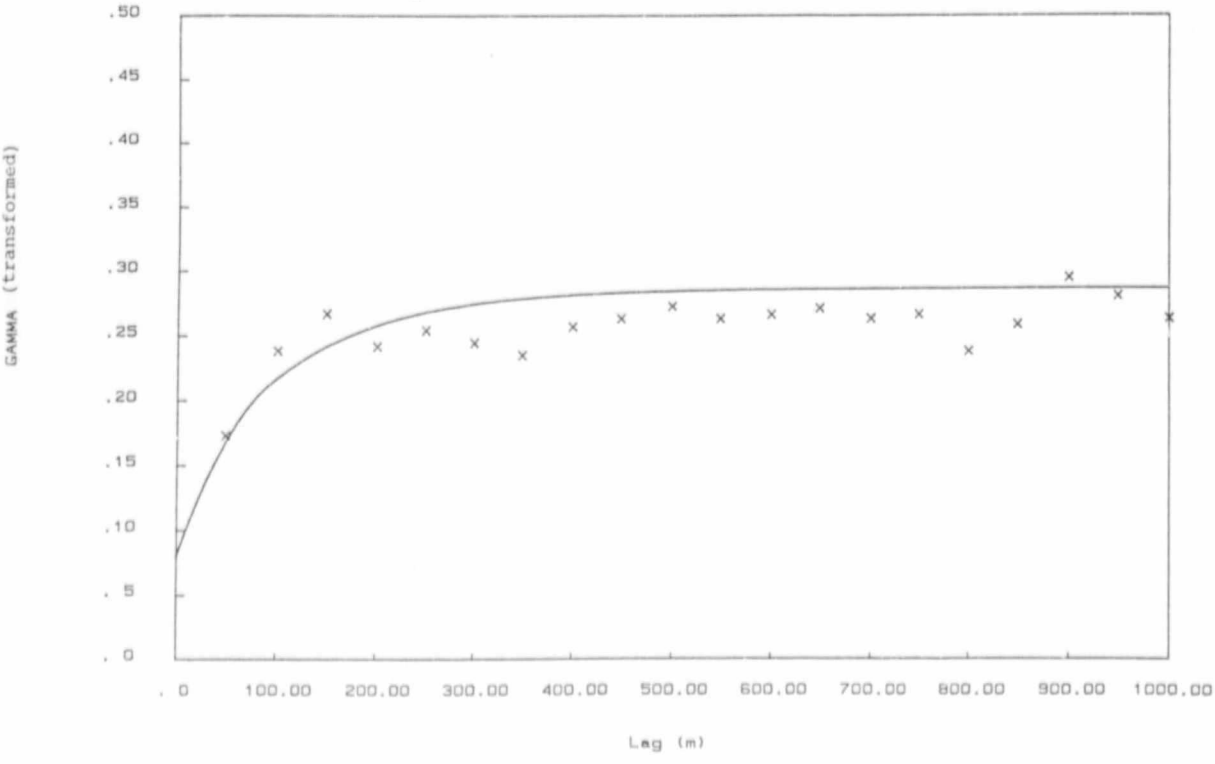
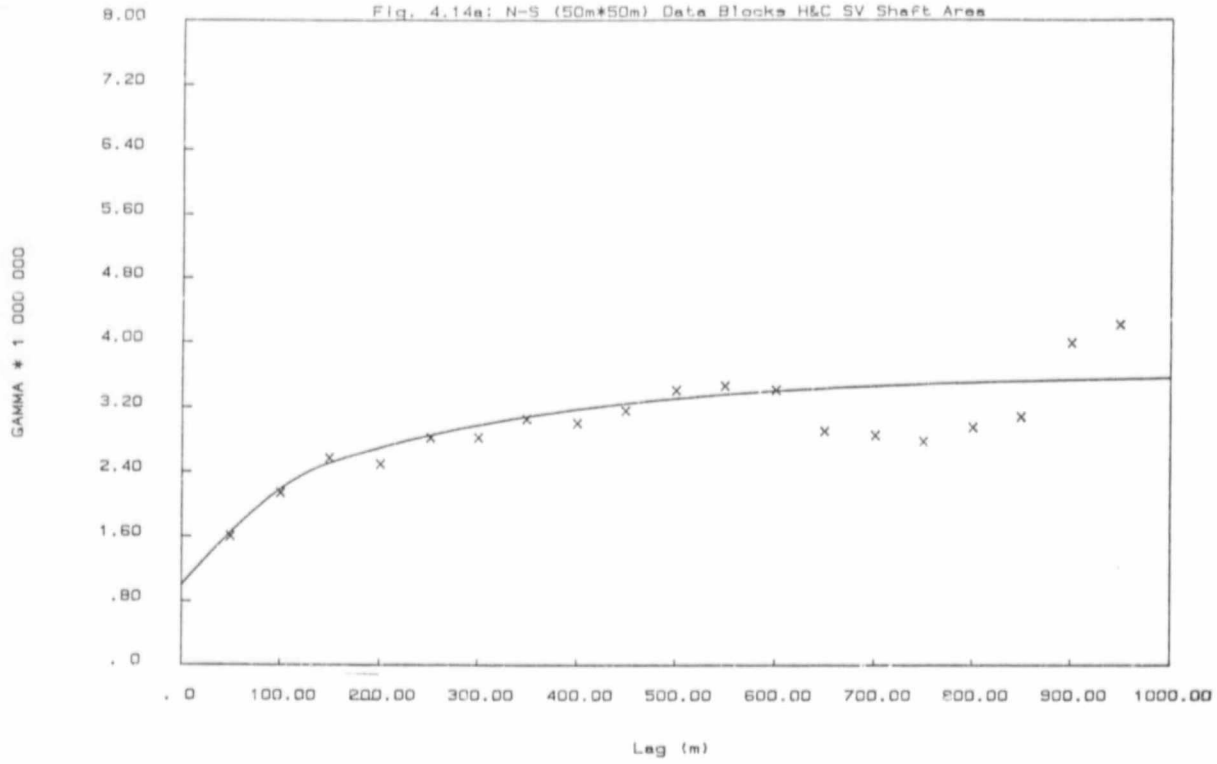
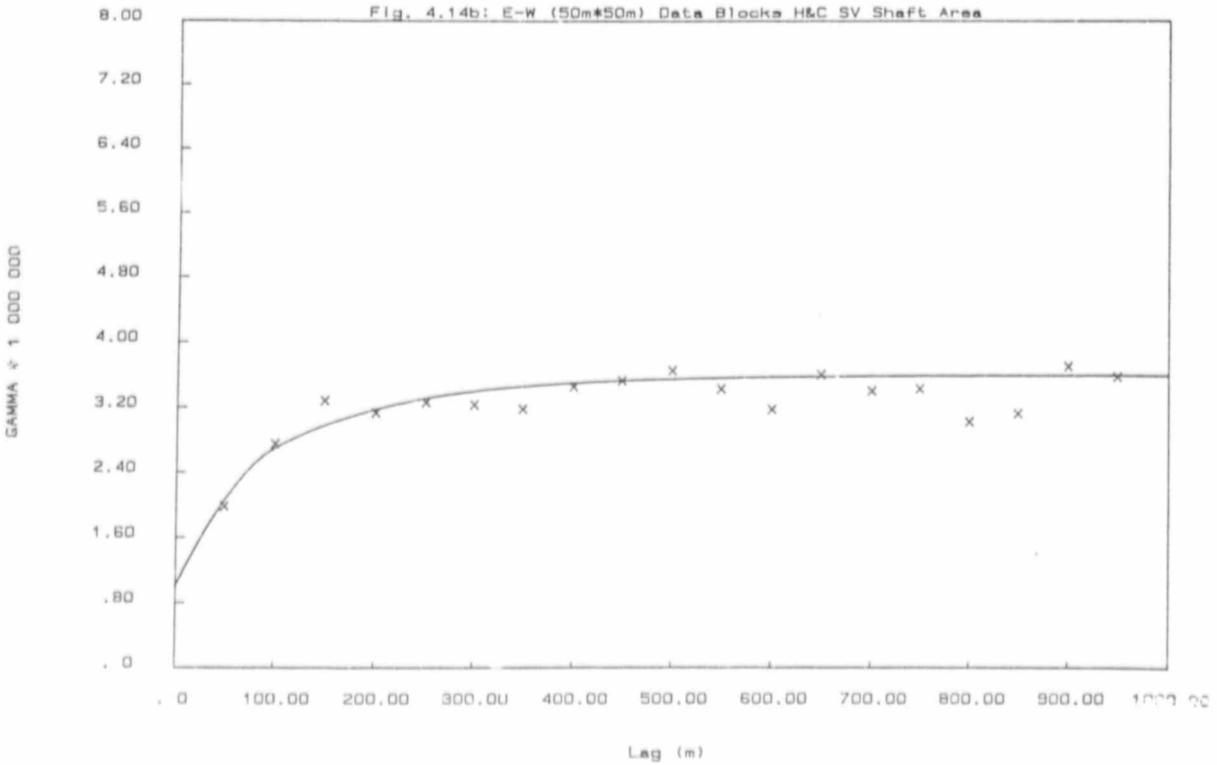
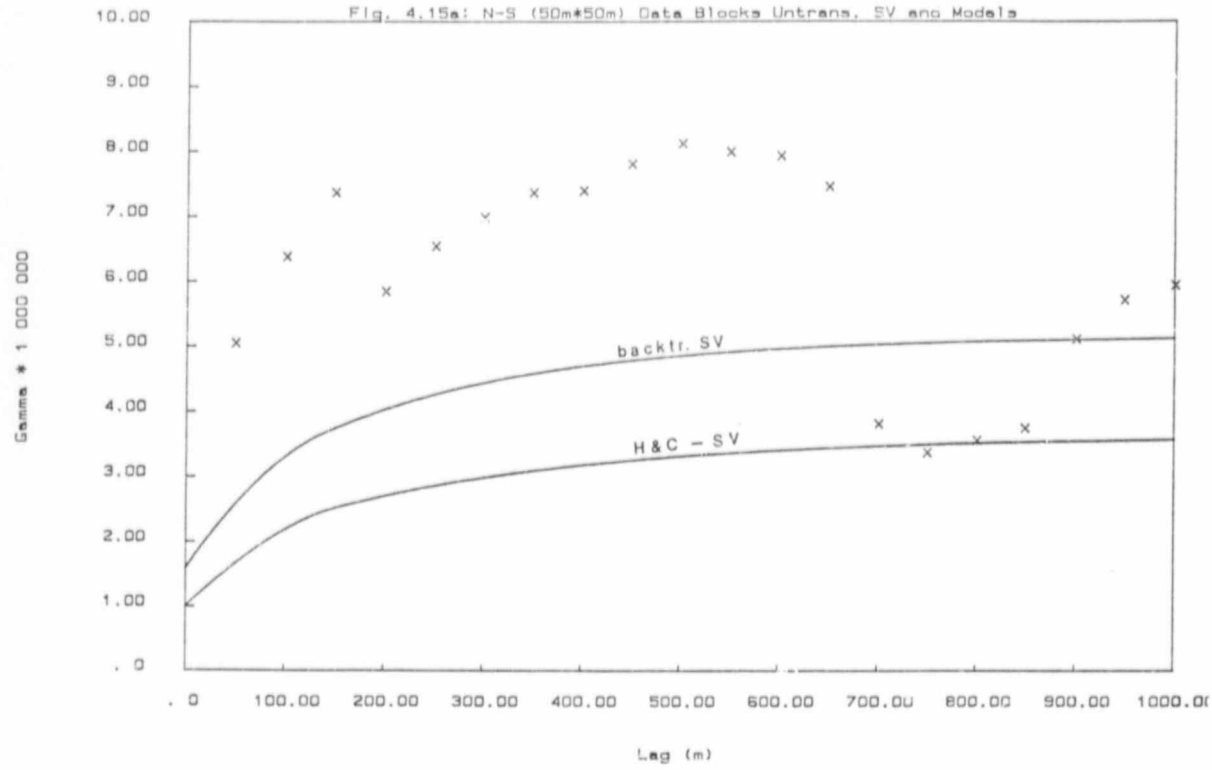


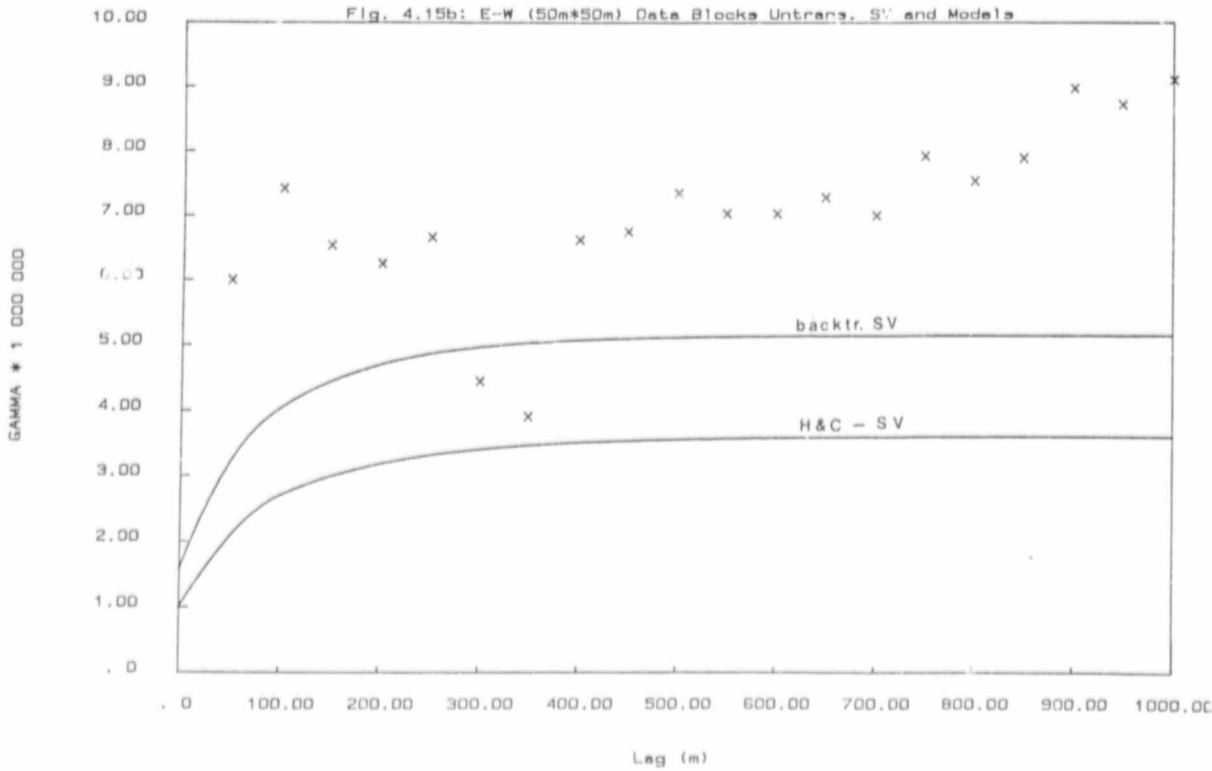
Fig. 4.13b: E-W (50m*50m) Data Blocks SV Shaft Area




Fig. 4.14a: N-S (50m*50m) Data Blocks H&C SV Shaft Area
GAMMA * 1 000 000
8.00
7.20
6.40
5.60
4.80
4.00
3.20
2.40
1.60
.80
. 0
. 0
100.00
200.00
300.00
400.00
500.00
600.00
700.00
800.00
900.00
1000.00
Lag (m)


Fig. 4.14b: E-W (50m*50m) Data Blocks H&C SV Shaft Area
GAMMA * 1 000 000
8.00
7.20
6.40
5.60
4.80
4.00
3.20
2.40
1.60
.80
. 0
. 0
100.00
200.00
300.00
400.00
500.00
600.00
700.00
800.00
900.00
Lag (m)


Fig. 4.15a: N-S (50m*50m) Data Blocks Untrans. SV and Models
Gamma * 1 000 000
10.00
9.00
8.00
7.00
6.00
5.00
4.00
3.00
2.00
1.00
. 0
backtr. SV
H&C – SV
. 0
100.00
200.00
300.00
400.00
500.00
600.00
700.00
800.00
900.00
1000.00
Lag (m)


Fig. 4.15b: E-W (50m*50m) Data Blocks Untrans. SV and Models
GAMMA * 1 000 000
10.00
9.00
8.00
7.00
5.00
4.00
3.00
2.00
1.00
. 0
backtr. SV
H&C – SV
. 0
100.00
200.00
300.00
400.00
500.00
600.00
700.00
800.00
900.00
1000.00
Lag (m)

effect of 32%. The backtransformed nugget effect is to be expected to be relatively higher than the logtransformed one (David, in print).

The ranges of all models are very similar. The overall sill of the backtransformed semivariogram is equal to the population variance of the data based on the logarithmic variance, which can be taken as the true population variance of the data undistorted by outliers. The overall sill of the Hawkins & Cressie transformed semivariogram is 12% lower.

The formula relating the population variance V^2 to the logarithmic variance LV_b^2 of the three - parameter lognormal model is (Krige, 1981):

$$V^2 = (\overline{Z} + b)^2 * (\exp(LV_b^2) - 1)$$

These regularized semivariogram models are used in the geostatistical ore reserve estimation techniques described in chapter 4.5.2.

4.5.2 Ore Reserve Estimation

The mining technique applied at Western Deep Levels Gold Mine is longwall mining due to the great depth. For that reason only data on one side of an oreblock are available to estimate the mean grade of that block:

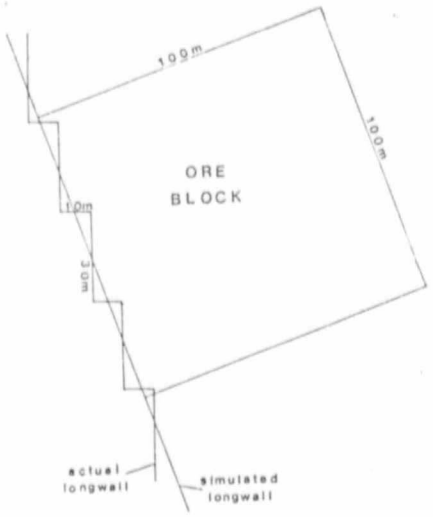


Figure 4.16a: Standard mining situation at time of ore block estimation, and simulated longwall position.

In reality the longwalls are not as regular as shown in Figure 4.16a, but in order to do the calculations automatically by computer, a regular setup had to be used. Moreover, for reasons of computing efficiency the longwall was simulated as a straight line, as illustrated in Figure 4.16a. This reduced the time required for the selection of the samples which were used for each ore block estimation by a factor of 5.

Only data in an area of $(500m)^2$ located on one side of the ore block - as illustrated in Figure 4.16b - are used in the estimation of that ore block.

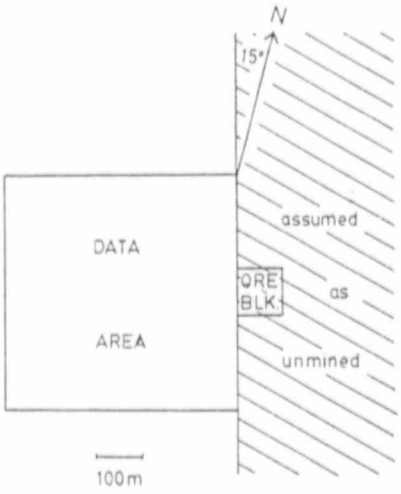


Figure 4.16b: Estimation set-up simulated for the longwall mining condition.

However, size ($(100m)^2$), shape and location of the ore blocks are identical with the ore block grid used by the mine.

The following different kriging methods have been tried (the theory of the different kriging methods is well documented in the geostatistical literature (e.g. Journel & Huijbregts, 1978; Rendu, 1979a, Rendu, 1979b, Dowd, 1982), and will not be repeated here):

untransformed data	logtransformed data
Simple Kriging	Simple Lognormal Kriging
Ordinary Kriging	Ordinary Lognormal Kriging
Universal Kriging	

In the case of both simple and simple lognormal kriging, much weight is given to the mean, therefore local means were also used instead of a global mean. The one way to calculate a local mean was to take all data blocks in the area of $(500m)^2$ on the one side of the oreblock, calculate their mean, and use this as local mean in the estimation.

The second method used was to fit a linear trend to the data within the $(500m)^2$ data block area. This trend was then extrapolated and a value indicated for an area of $(300m)^2$ centered at the oreblock was used as a local mean. As this method gives some unrealistic high as well as some negative local means, upper and lower limits were imposed. The upper and lower 5% confidence limits of the distribution of the $(300m)^2$ blocks of each subarea were applied as limits to the estimates of the local mean.

Only a linear trend was calculated, as trend surfaces of higher orders give unrealistic estimates in most of the cases. This is a general problem with the sample

setup under longwall mining conditions, where all predictions are based on extrapolation rather than interpolation. This problem was also found in using universal kriging.

The author's computer programs 'UKSIM' and 'UKSIMTR' (see Appendix 2.6 and 2.7) select the samples inside the data area , and use only these samples for the estimation of the oreblock (see Figure 4.16b). This pattern is moved over the whole mined out area.

Using $(50m)^2$ data blocks within the $(500m)^2$ data area, an ore reserve estimation was simulated for different logtransformed and untransformed kriging variations. In the case of untransformed kriging, both a Hawkins & and Cressie semivariogram and a backtransformed semivariogram (see Appendix 1.2) were used (see Figures 4.13 to 4.15). The following abbreviations will be used for the different methods:

Lognormal kriging:

SLK-GM: simple lognormal kriging - global mean
SLK-ST: simplelognormal kriging- local mean
(mean of data area)
SLK-LT: simple lognormal kriging - local mean
(linear trend)
OLK : ordinary lognormal kriging

Untransformed kriging - backtransformed semivariogram:

SBK-GM: simple kriging - global mean
SBK-ST: simple kriging - local mean
(mean of data area)
SBK-LT: simple kriging - local mean
(linear trend)
OBK : ordinary kriging

UBK : universal kriging (linear trend)

Untransformed kriging - Hawkins & Cressie semi-variogram:

SHK-GM: simple kriging - global mean
SHK-ST: simple kriging - local mean
(mean of data area)
SHK-LT: simple kriging - local mean
(linear trend)
OHK : ordinary kriging
UHK : universal kriging (linear trend)

If subdivision is ignored, the shaft area mean is taken as the global mean. With subdivision, the subarea mean is used as global mean.

These fourteen methods give fourteen sets of estimates which can be compared with follow-up data. Each set consists of 305 pairs of estimates and 'true' grades. Oreblocks had to contain at least 40 samples to qualify as 'true' oreblocks (see Figure A1.2).

4.5.3 Analysis of Simulation

A linear regression analysis of each of the fourteen sets of estimated and follow-up grades gives the slope of the regression line, and an actual error variance. These two parameters are plotted in an X-Y scatter plot in Figures 4.17a and b. (The complete regression results are given in Table 4.1.) The standard error of the slope is plotted as a horizontal bar on each side of the asterisks. Untransformed error variances were transferred into their logtransformed equivalents to make them comparable.

The general results of this simulation are:

- Universal kriging gives the worst estimates. The slope factors are furthest away from 1.0, and the observed error variances are highest. This shows the difficulties in extrapolating a trend ahead of the face.

- The quality of the estimation of the block grades is the same using either a Hawkins & Cressie or a back-transformed semivariogram.

- On an untransformed basis, ordinary kriging and simple kriging with local means calculated from the data area give very similar results, while simple kriging using a local mean calculated on an extrapolated linear trend yields slighlly better estimates.

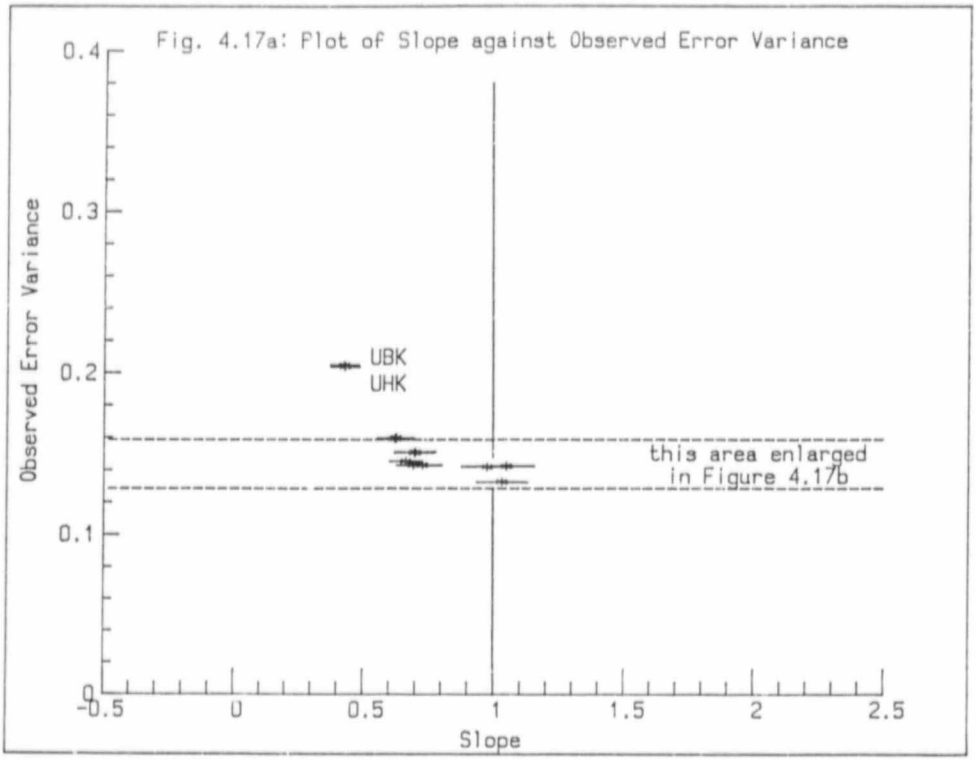
- The mean errors of the individual methods (Z^*-Z) are close enough to zero to consider all kriging variations as being globally unbiased.

- Lognormal kriging tends to give lower error variances for the same methods.

- However, only simple kriging with a global mean , either linear or logtransformed, gives conditionally unbiased results. All other methods are conditionally biased, and a slope factor of 1.0 is out of the range of even two or three standard deviations for all these cases.

In Figure 4.18, the estimation variance is plotted against the observed error variance. Because of the use of regularized data blocks, the sample setup and therefore also the estimation variance remains constant or virtually so for the main method groupings.

Except for universal kriging, the estimation variance underestimates the observed error variance. This error is between 24% and 88%. This is due to the non-stationarity of the overall semivariogram, as will be shown later (see chapter 4.8), and of course to the error made in assuming that the 'true' grades of the $(100m)^2$ ore blocks are known. Therefore the estimation error is no accurate measurement of the actual accuracy of the estimation.


Fig. 4.17a: Plot of Slope against Observed Error Variance
Observed Error Variance
0.4
0.3
0.2
0.1
0
UBK
UHK
this area enlarged
in Figure 4.17b
-0.5
0
0.5
1
1.5
2
2.5
Slope

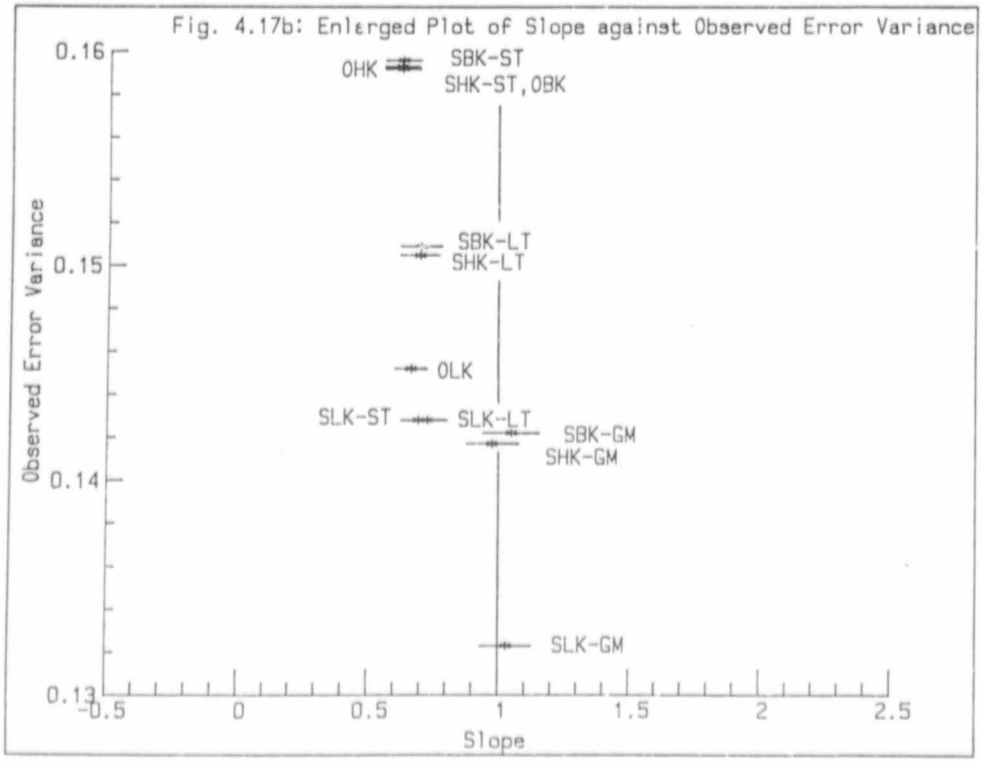
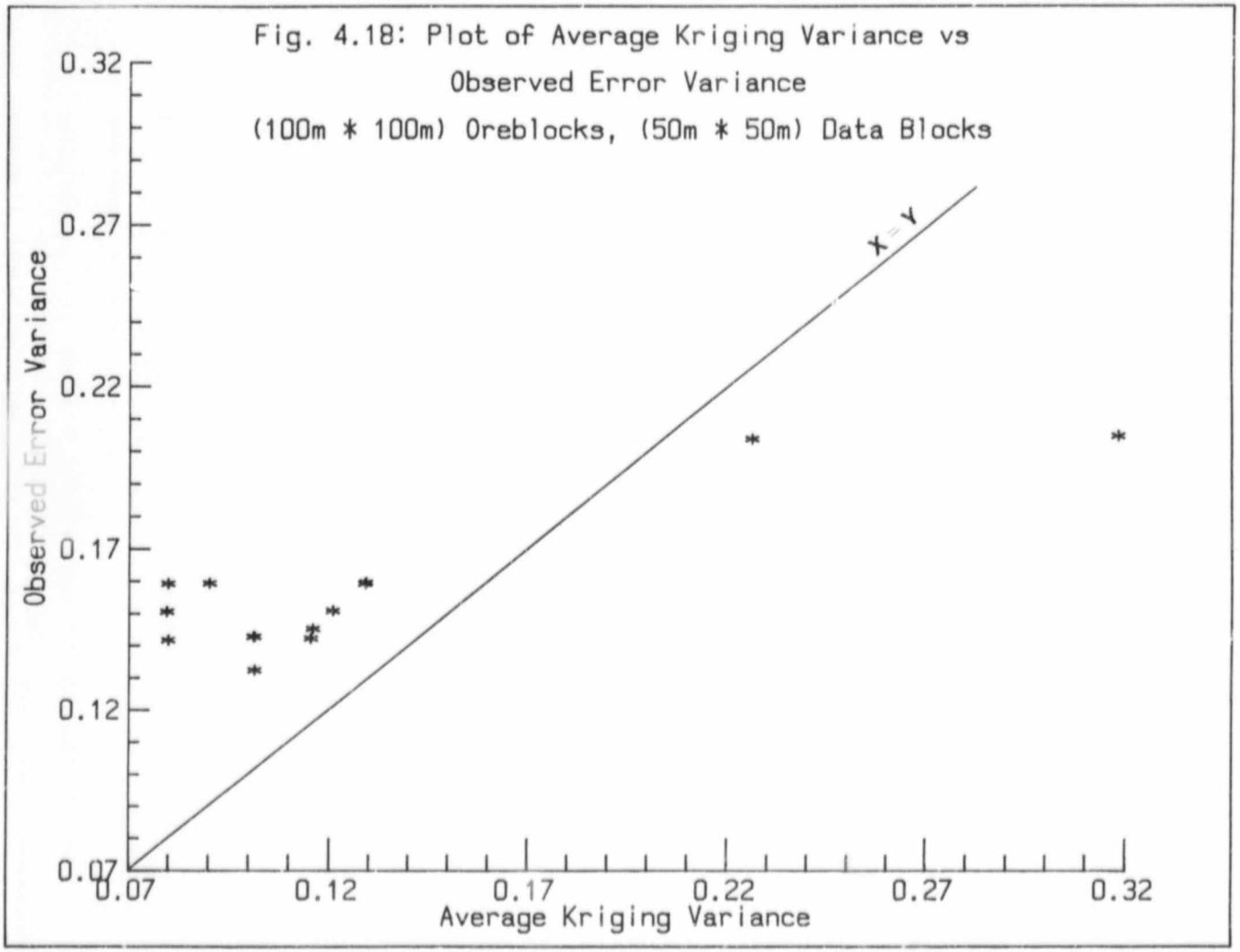

Fig. 4.17b: Enlarged Plot of Slope against Observed Error Variance
Observed Error Variance
0.16
0.15
0.14
0.13
OHK
SBK-ST
SHK-ST, OBK
SBK-LT
SHK-LT
OLK
SLK-ST
SLK-LT
SBK-GM
SHK-GM
SLK-GM
-0.5
0
0.5
1
1.5
2
2.5
Slope

Table 4.1: Shaft area, regression analysis of 305 $(100m)^2$ ore blocks by $(50m)^2$ data blocks.

method	regression formula $\ln(Z + b) / Z =$	standard error of slope	corrected/ transformed error variance actual	corrected/ transformed error variance estimated by kriging	$\bar{Z}^* - \bar{Z}$ in %
SLKGM	$-0.28 + 1.0290 \ln(Z^*+170)$	.0963	.13239	.10141	-1.9
SLKST	$2.52 + .6902 \ln(Z^*+170)$	.0651	.14279	.10141	0.1
SLKLT	$2.23 + .7249 \ln(Z^*+170)$	.0739	.14276	.10108	1.3
OLK	$2.75 + .6610 \ln(Z^*+170)$	.0617	.14522	.11588	2.4
SBKGM	$-91 + 1.0450\ Z^*$	.1061	.13991	.11542	2.1
SBKST	$1426 + .6245\ Z^*$	.0672	.15962	.12919	-0.9
SBKLT	$1203 + .6979\ Z^*$	.0775	.15092	.12090	-2.2
OBK	$1465 + .6229\ Z^*$	.0659	.15922	.12886	1.2
UBK	$2245 + .4250\ Z^*$	.0540	.20459	.19823	-4.1
SHKGM	$196 + .9735\ Z^*$	.0981	.14169	.07980	-2.6
SHKST	$1462 + .6232\ Z^*$	.0661	.15923	.07980	-1.1
SHKLT	$1225 + .6937\ Z^*$	.0759	.15050	.07980	-2.5
OHK	$1484 + .6192\ Z^*$	.0649	.15928	.09013	-1.4
UHK	$2235 + .4283\ Z^*$	.0537	.20371	.20126	-4.2


Fig. 4.18: Plot of Average Kriging Variance vs
Observed Error Variance
(100m * 100m) Oreblocks, (50m * 50m) Data Blocks
Observed Error Variance
0.32
0.27
0.22
0.17
0.12
0.07
X=Y
0.07
0.12
0.17
0.22
0.27
0.32
Average Kriging Variance

4.6 Subdivision of Study Area

4.6.1 Basic considerations

As the ore control of the Carbon Leader reef is sedimentary, a geostatistical analysis which considers the sedimentology is expected to give improved results. The inclusion of qualitative and semiquantitative geological information into the numerical estimation process will not be attempted. Geology is therefore used to subdivide the area under investigation into geostatistically homogeneous zones with a similar variability and spatial structure of the ore in each zone.

The criteria for subdividing should be selected with practicality in mind. It will be of advantage if the subdivisions could be determined on a straightforward routine basis; it is essential that extrapolation of the zones into the unmined areas can be effected with reasonable accuracy.

Furthermore, the zones should neither be too small, as the data will be inadequate for the semivariogram calculation; nor should the zones be so large that an overall semivariogram does not allow for local changes in variability.

In the case of the Carbon Leader reef a subdivision into Subfacies 1 areas and Subfacies 2 areas is advisable.

Because of the different depositional processes the two reef types are expected to have different variability patterns; as the palaeochannels seem to be fairly linear, their courses can be extrapolated into unmined areas. With widths of 200m and more the zones are large enough to allow calculations of reliable semivariograms for use in the block estimation process.

4.6.2 Geostatistical characteristics of the different subfacies

Five of the subareas are sufficiently mined out to give each a sufficient number of samples in each subarea for follow-up analyses.

Two subareas are of Subfacies 1 type, and are located in the southern quadrants. The other three are of the Subfacies 2 type; one of which lies in the southeastern quadrant, and the remaining two in the northwestern quadrant.

Table 4.2: Basic statistics of five subpopulations. (Values from individual sample sections).

	Z (+ constant)	b	Skew-ness	n	LV^2	CoV
S11	5752	211	-.00007	1575	1.2071	2.3437
S12	4306	112	.00080	3996	1.1004	2.0034
S21	5983	171	.00050	9404	.9838	1.6746
S22	5020	230	-.00050	4611	.7474	1.1115
S23	6136	289	-.00050	5519	1.0305	1.8025

S1.1: Subfacies 1, subarea 1; S1.2: Subfacies 1, subarea 2
S2.1: Subfacies 2, subarea 1; S2.2: Subfacies 2, subarea 2
S2.3: Subfacies 2, subarea 3
b : additive constant n: number of samples
CoV: coefficient of variation = $V^2/Z^2 = \exp(LV^2)-1$ (for log-normal case).
LV^2: log.variance of corresponding two parameter lognormal model, corrected for b.

The grades of all subareas follow a three parameter lognormal model. The basic statistical parameters are listed in Table 4.2.

The plots of the five subpopulations on logarithmic probability paper are shown in Figures 4.19 to 4.23.

It can be seen that the difference in grades between the two subfacies is not as significant as the difference in their variability, as expressed by the coefficient of variation. The variability of the gold grades is higher in subfacies 1 subareas than in subfacies 2 areas. This was discovered by Nami as well in an area northwest of the study area. In both subfacies there is a proportional effect present, in spite of taking logarithms of the values. This can happen in Witwatersrand gold reefs (Rendu, 1978).

In kriging, the semivariogram model is used to compute covariances during the estimation process. A model is based on experimental semivariogram values calculated from the available data for a range of lag distances. It is generally acknowledged that the modelling of a semivariogram is one of the more difficult tasks in the ore estimation process (e.g. Armstrong,1984). It is here where personal judgement is involved, and two geostatistians are most likely to fit (slightly?) different models to the same experimental semivariograms.

The author admits the influence of the geological interpretation on his choice of semivariogram models. Other models might be equally valid. A check of the finally chosen models against their variance - size of area graphs (in the logtransformed case), however, reveals that the maximal deviation between model and reality is 4.7% for subfacies 1, and 2.7% for subfacies 2 subareas.

Semivariograms for the five subareas, and the variance - size of area graphs (both calculated from the logtransformed semivariogram models and from the sample data), are shown in Figures 4.24 to 4.33.

Both semivariograms for the Subfacies 1 type areas show a geometric anisotropy with a weaker structure in east - west direction. The main axes of anisotropy correspond with the north - south palaeoflow direction. This type of geometric anisotropy can be expected in channelized sediments, and sedimentary river deposits serve as examples of geometric anisotropies in geostatistical textbooks (e.g. Journel & Huijbregts, 1978).

For subarea S1.1 a trend in the data in north - south direction is indicated by the rising of the calculated semivariogram beyond the variance. As this happens only

beyond the range of the semivariogram, it is neglected for the estimation, and the fitted model is of the transition type, as for the other subareas.

Both semivariograms for the Subfacies 1 - type subareas show a cyclicity in east - west direction, with lower semivariances at lag distances of 30m, 125m and 190m. While the two larger intervals could not be related to the sedimentology, it is interesting to note that the east - west extension of the gravel bars, as described in chapter 3.3, is about 30m. As these gravel bars influence the water flow in the channel, they have an influence on the distribution of the gold grains, which are transported both in suspension and as bedload (James,1984).

Directional semivariograms of Subfacies 2 - subareas are so similar that isotropy of the spatial variability can be assumed. Moreover, whereas a river is expected to distribute heavy minerals anisotropically (Subfacies 1 type), the geological model of a slowly transgressing sea (Subfacies 2 type), which concentrates the heavy minerals in the swash zone, suggests an isotropic continuity of the mineralisation.

The fitted models consisted in all cases of nested structures: a nugget effect of 40% to 61%, a spherical model with a relative short range to accommodate the steep increase in variability for short lags, and an exponential model with a larger range, which then eventually reaches the sill of the semivariogram. In all cases, the sill was chosen as equal to the logarithmic variance of the data within the subarea.

Table 4.3 shows some semivariogram features of the two subfacies types for comparison.

Table 4.3: Comparison of logtransformed semivariogram models of subfacies ('point models').

	% C0	C2/C1	A1		A2		Equivalent Sill for b = 0.
			N-S	E-W	N-S	E-W	
S11	40	3.60	20	15	60	30	1.2071
S12	53	3.31	20	10	100	20	1.1004
S21	49	.98	15	15	50	50	.9838
S22	50	1.12	10	10	48	48	.7474
S23	61	.86	15	15	40	40	1.0305

The ratio of the sill of the second (exponential) structure to the first (spherical) structure is about 3.5 in Subfacies 1, while the two sills are approximately equal in Subfacies 2.

The ranges of the first, spherical structures range from 10m to 20m for both subfacies types, and do not differ substantially. For the exponential, second structure, however, the ranges of the isotropic Subfacies 2 are roughly halfway between the minimum and maximum ranges of the anisotropic Subfacies 1.

In the author's opinion, this is due to the equalizing effect the transgressional process, which created Subfacies 2, had on the gold brought in by the rivers. The high directional order of the mineralisation as created by the rivers got destroyed once the gold had been redistributed by the sea. The lower overall logarithmic variance of Subfacies 2 areas is also attributed to its more homogeneous origin.

Figures 4.34a to 4.34c picture the semivariogram models fitted to the logtransformed, backtransformed, and Hawkins & Cressie transformed experimental semivariograms of the five subareas, and the shaft area.

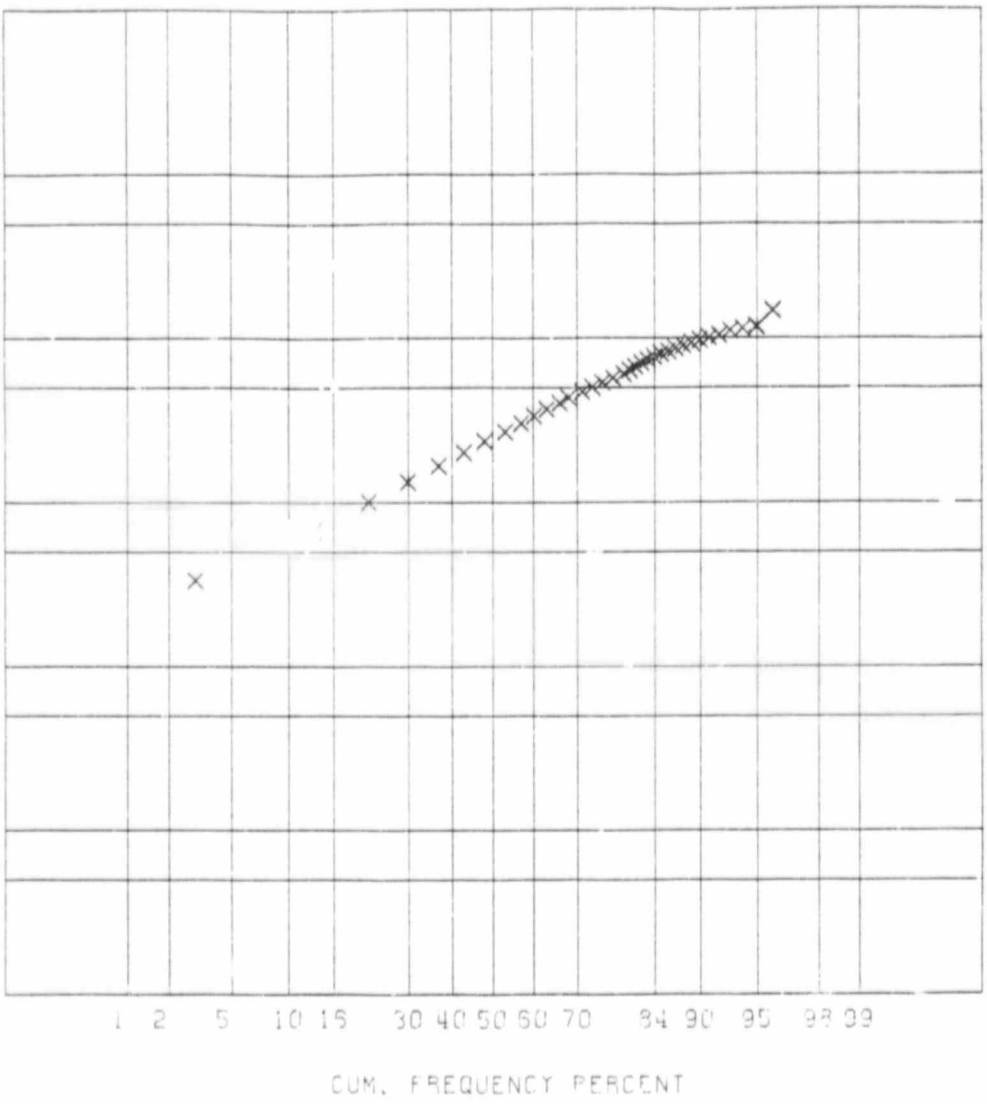
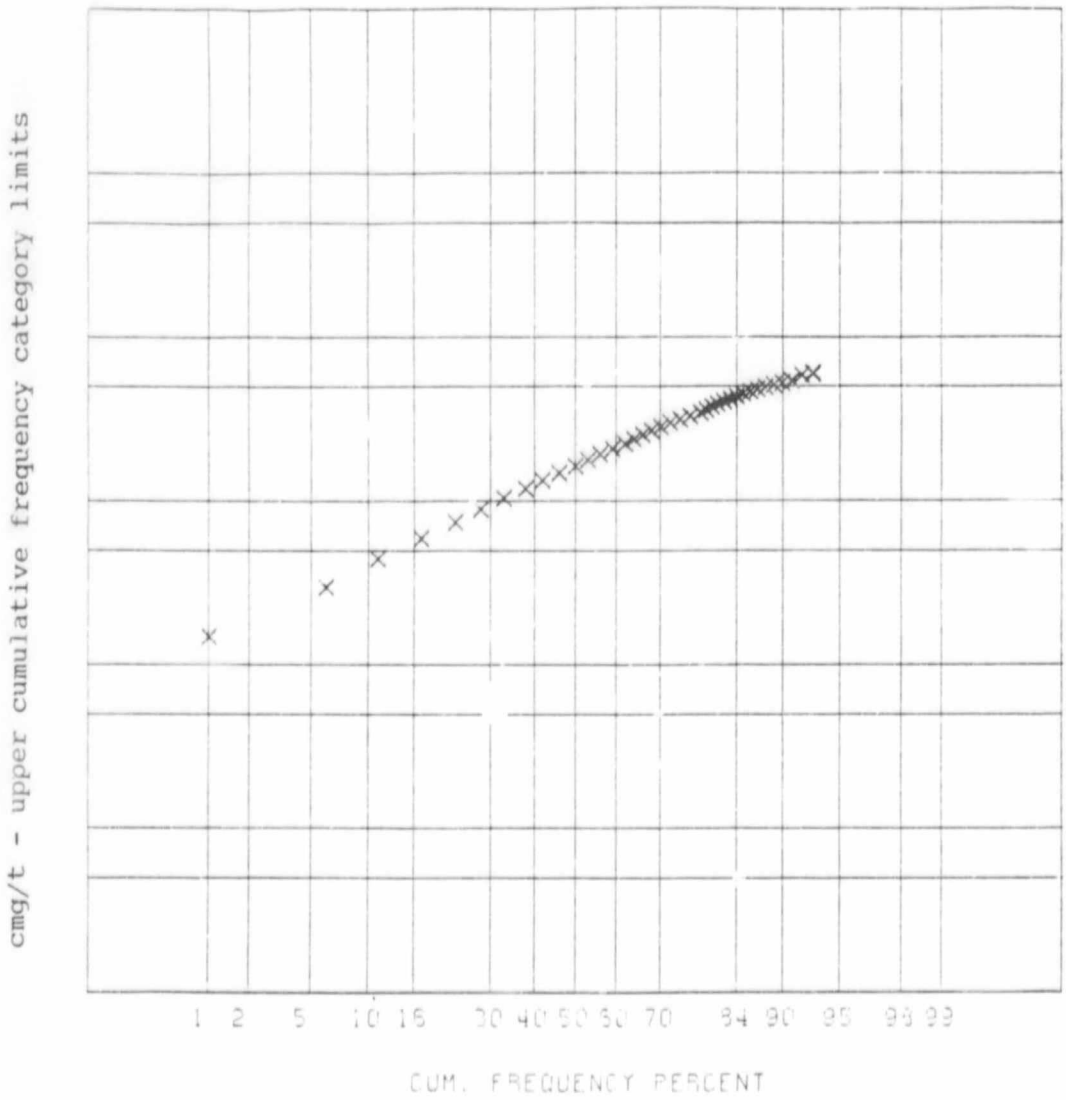


Figure 4.19: Logarithmic probability plot of 1575 chip samples of subarea S1.1 .



× = ACTUAL VALUES + CONST.
ARITHM. MEAN=
GEOM. MEAN=
SICHELS T-ESTIMATOR
VARIANCE= 19029934.0
LOG. VARIANCE= 1.056
STD. DEV.= 4362.335
NUMBER OF SAMPLES= 3996
ADD. CONSTANT= 112.000

Figure 4.20: Logarithmic probability plot of 3996 chip samples of subarea S1.2 .

Author Braun Rolf
Name of thesis A Study To Optimize Ore Evaluation At Western Deep Levels Gold Mine, Witwatersrand, By Using Geostatistics And Geological Subdivision. 1988

PUBLISHER:
University of the Witwatersrand, Johannesburg
©2013

LEGAL NOTICES:

Copyright Notice: All materials on the University of the Witwatersrand, Johannesburg Library website are protected by South African copyright law and may not be distributed, transmitted, displayed, or otherwise published in any format, without the prior written permission of the copyright owner.

Disclaimer and Terms of Use: Provided that you maintain all copyright and other notices contained therein, you may download material (one machine readable copy and one print copy per page) for your personal and/or educational non-commercial use only.

The University of the Witwatersrand, Johannesburg, is not responsible for any errors or omissions and excludes any and all liability for any errors in or omissions from the information on the Library website.